

## Authors' Response

### Referee #1

This is an interesting paper about structured and well-described experiments on the cyclic loading of saline ice. In this work, novel and apparent test setup is used for testing of floating ice in the laboratory. Saline ice is produced in the laboratory in an unusual way and, surprisingly, showed a microstructure very similar to that of S2 sea ice. The growing and preparation method ensures that ice structure and the presence of brine in ice are not affected until the experiment begins. A fair amount of discussion is presented concerning the earlier work, suggesting reasons for the need in the testing of floating wet ice samples. The behavior of ice upon cycling is well predicted by the model. The key point of the paper is that warm wet floating ice behaves differently from cold dry ice. A weakness of the paper is that there is no clear answer/evidence on whether both water and temperature or only temperature play a major role in the mechanical behavior of ice under cyclic loading.

Overall, the paper is clearly written and provides new results. It is worthy of publication once some details have been clarified.

**Re: We sincerely thank the reviewer for the constructive comments and valuable time devoted to improving our manuscript. We have modified our manuscript according to the comments. The majority of them lead to modifications.**

### Specific comments:

1. Please, state that the sinusoidal waveform was used during cycling in the abstract (line 13) and introduction (line 61) for the readers' convenience. For example, "stresscontrolled sinusoidal cyclic compression experiments" (lines 13-14).

**Re: Thanks for the comment. We have made the corresponding changes in the revised manuscript.**

**Lines 13 and 14, "stress-controlled sinusoidal cyclic compression experiments"**

**Line 60, "stress-controlled sinusoidal cyclic compression experiments"**

2. Lines 38-39: A reference to the study of ice fatigue in-situ tests led by Langhorne shall be provided. For example: \* Bond PE and Langhorne PJ (1997) Fatigue behavior of cantilever beams of saline ice. J. Cold Reg. Eng. 11(2), 99-112; \* Haskell TG, Robinson WH and Langhorne PJ (1996) Preliminary results from fatigue tests on in situ sea ice beams. Cold Reg. Sci. Technol. 24(2), 167-176 \* Langhorne PJ, Squire VA, Fox C and Haskell TG (1998) Break-up of sea ice by ocean waves. Ann. Glaciol. 27, 438-442.

**Re: We thank the reviewer for pointing this out. Corresponding changes have been made in the revised manuscript.**

**Line 37, "...give insight into the fatigue of ice (Bond and Langhorne, 1997; Langhorne et al.,1998...)"**

3. Lines 40-42: Strictly speaking, first cyclic loading experiments on freshwater ice were conducted in the forties: Kartashkin B.D., 1947. Experimental studies of the physico-mechanical properties of ice. Similarly, experiments on sea ice were firstly performed in the eighties: Tabata T, Nohguchi Y, 1980. Failure of sea ice by repeated compression.

**Re: The literature review has been modified in the revised manuscript.**

**Lines 40 and 41, "...have been performed since the forties (Kartashkin, 1947; Mellor and Cole, 1981) and on saline ice since the eighties (Tabata and Nohguchi, 1980...)"**

4. Lines 54-57: Reference to in-situ experiments by Langhorne shall be provided.

Re: Three pieces of literature by Langhorne, related to in-situ experiments, have been added in the revised manuscript.

Line 55, "...in-situ experiments on floating ice (Langhorne et al., 2015; Smith et al., 2015; Wongpan et al., 2018)"

5. Lines 92-93: What was the reason for the temperature to be changed twice?

Re: Lower temperature (-14°C) was used for practical reason: make the ice grow faster. This was then changed to -10°C to perform the tests in a temperature such tests are often performed. The change was done well ahead of the actual experiments to ensure that the ice used for floating experiments had stable temperature and thermal gradient. We did not notice differences in the ice structure due to the change.

6. Line 99: What does "about" mean? Can authors provide standard deviation or standard error for their measurements?

Re: The standard deviations for the density measurements have been provided in the revised manuscript.

Line 88, "...and their densities were  $886 \pm 19$  and  $879 \pm 16 \text{ kg} \cdot \text{m}^{-3}$ , respectively"

7. Line 127: What was the accuracy of temperature measurements? Thermistors and thermocouples usually have an accuracy in the range from about  $\pm 0.3$  to  $\pm 2.5^\circ\text{C}$ . In this case, the resolution is not important for the manuscript and shall be replaced with accuracy.

Re: We agree. The accuracy of temperature measurements was  $\pm 0.5^\circ\text{C}$ . This information has been supplemented in the revised manuscript. Thanks for this constructive comment.

Line 112, "...and an accuracy of  $\pm 0.5^\circ\text{C}$ "

8. Line 137: Again, what is the accuracy of LVDT? Is it more important than a resolution?

Re: The description has been updated in the revised manuscript (line 144). We agree that the accuracy of LVDT (0.001 mm) is more important than the resolution (0.0001 mm). The "resolution" described in the original manuscript was actually referring to the "accuracy". Apologies for this clerical error.

Line 120, "...with a measurement range and accuracy of 2 and  $\pm 0.001$  mm, respectively"

9. The stress during cycling was as low as 0.005-0.085 MPa (line 327). This range seems to be very low. What was the accuracy of a load cell and how accurate the machine (actuator) could control load-limits? Could the test setup ensure accurate cycling between 0.005 and 0.085 MPa? This should be commented on in the text.

Re: We have modified the text to comment on this. Since the specimen size was  $0.6 \text{ m} \times 0.3 \text{ m} \times 0.1 \text{ m}$ , the force applied for stress amplitude 0.005–0.085 MPa was 0.15–2.55 kN. The accuracy of the load cell was  $\pm 5 \text{ N}$ ; thus, there was no severe error on the cyclic stress values and we have a reason to assume that the cycling was accurate.

Line 106, "The load cell had an accuracy of  $\pm 5 \text{ N}$ , which is sufficient for all stress levels and cycles of the experiments here"

Line 304, "Nominal cyclic stress of 0.005–0.085 MPa is low, but the setup could achieve it: With the accuracy of the system, the actual stress applied to the specimen was 0.005 ( $\pm 0.001$ )–0.085 ( $\pm 0.003$ ) MPa"

10. When using words "linear loading" you always should be careful since ice never behaves purely elastically (linearly); an inelastic component (though minor) is always present.

Re: We agree. The statement was actually referring to the application of a linear loading ramp, not the response of the ice. For clarity, the related sentences have been modified as follows.

Line 144, “the duration of the initial loading ramp was fixed to be 1 s”

11. Lines 212-213: References to other works that show similarly that the hysteresis loop area increases with an increase of the cyclic period shall be added: \* Weber LJ and Nixon WA (1996) Hysteretic Behavior in Ice Under Fatigue Loading. Proceedings of the 15th International Conference on Offshore Mechanics and Arctic Engineering. 75–82 \* Murdza A, Schulson EM and Renshaw CE (2018) Hysteretic behavior of freshwater ice under cyclic loading: A preliminary results. 24th IAHR International Symposium on Ice. Vladivostok, 185–192 \* Cole DM (1990) Reversed direct-stress testing of ice: Initial experimental results and analysis. Cold Reg. Sci. Technol. 18(3), 303–321.

Re: Missing references have been added in the revised manuscript.

Line 187, “...consistent with earlier studies (Cole, 1990; Murdza et al., 2018; Weber and Nixon, 1996)”

12. It is mentioned in Lines 208-211 that the area of the hysteresis loop is decreasing until a “steady-state” is reached. Does this happen only during the first set of loading ( $T=1s$ ) or during any subsequent loadings as well? (especially after 15 min of recovery in the case of dry ice)? If some cycles are needed to reach a steady-state condition every time (for example after relaxation) then is  $N=4$  cycles at  $T=1000s$  for dry ice and  $N=1$  cycle for wet ice enough to get a steady-state as mentioned in line 225?

Re: In brief, the phenomenon happened in all the dry experiments. However, the larger the  $T$  value, the less the number of cycles required to reach the “steady-state”. This is shown by Figure 9, in which there are 5 or 6 cycles before the experiment with  $T = 100$  s reaches the “steady-state”, while the experiments with  $T = 500$  and  $1000$  s only require two cycles and one cycle, respectively, to achieve the “steady-state”. An important reason why the dry specimens require some cycles to reach the “steady-state” is the 15-minute recovery period before each experiment. In the floating ice experiments, the cyclic loads with increasing periods were applied to the specimen in a continuous manner – loading with one period after another without a recovery period. After some initial loading cycles of  $T = 1$  s, the ice samples maintained a relatively steady state in subsequent cyclic loads (Figures 10 and 11). For example, the areas of the two hysteresis loops at  $T = 100$  s are very similar, having a much smaller difference than those of the first two hysteresis loops in the dry experiments with  $T = 100$  s. Therefore, it is believed that  $N = 1$  can be used for the floating experiment with  $T = 1000$  s. In addition, the good agreement between the experimental and modeling results also shows the reliability of the experimental scheme and test results to a certain extent. We have modified the text to discuss this, as shown below.

Line 183, “For example, the hysteresis loops after the first stress cycle in the dry experiment with  $T = 1000$  s are similar;  $N = 4$  is enough for the dry specimen at  $T = 1000$  s to show steady-state response”

13. It is emphasized through the manuscript on the importance of considering warm floating ice for the experiments, in contrast to cold dry ice. In addition, the conclusion that water and temperature have a greater effect on elastic modulus than salinity is made. It is not a big surprise that “warm” ice behaves differently than “cold” ice and the temperature of ice affects elastic modulus. Therefore, do you think that if you repeat your experiments on dry ice at about  $-2.5^{\circ}C$  (average temperature of wet specimens based on line 153) instead of  $-10^{\circ}C$  it would behave similarly to wet specimens? In this case, no additional brine will freeze during the storage as mentioned in line 410. Is it possible that brine migration during cycling affects mechanical properties? Perhaps, there is no need to conduct experiments on floating ice but rather increase the ice temperature. If authors think similarly, they should state it more clear because the reader

may get the impression that both floating and warm conditions are equally important during cyclic loading of ice (which may not be true). I think it would be interesting to compare the results of both wet and dry ice of similar temperatures.

Re: Earlier laboratory work on ice has mostly focused on dry, cold and isothermal ice. Here we wish to draw attention to the fact, that the results from such experiments may not apply directly on saline ice in its natural conditions, that is, when ice is floating in water – and also to the fact, that the experiments where this type of conditions are mimicked in the laboratory can be performed. We do not aim to differentiate between the importance of the different factors on the ice behavior and hope this is now more clearly stated in the manuscript. In brief, our goal was (i) to present our methods used to perform laboratory-scale experiments on ice in its natural conditions and validate their applicability with floating ice experiments and commonly used test conditions (dry experiments), (ii) to report experimental results from cyclic loading tests on floating and dry specimens using different salinities, stress amplitude and loading-unloading periods, and (iii) to analyze the test results of the floating ice and dry ice specimens using a physically based model.

Thus, the original intention of this study is not to investigate the effect of temperature and floating condition on ice behavior. Probably the previous version of our manuscript made some excessive comparisons between warm floating ice and cold dry ice and some sentences were somewhat misleading in that regard. The revised manuscript clarifies our goals. For example, we reorganized the conclusions around the two themes of this article: experimental methods and material modeling of floating ice. We also avoided using “wet experiments” to refer to the floating ice experiments, in order to avoid the misunderstanding that here we are studying the effect of water on ice behavior. We thank the reviewer this constructive comment.

Comparing the results of both wet and dry “warm” ice of would be interesting, but would need another extensive experimental campaign. Inspired by the comments by the reviewer, we plan to conduct experiments on this in our future work. In fact, research on the effect of water is scarce, which also shows the necessity of developing experimental equipment for floating ice tests (as done here), which will help to reveal the mechanical properties of floating ice more deeply in the future.

14. Generally, a paper should be short and laconic but “full” in context. I suggest the authors make their manuscript shorter where it is possible by removing unnecessary parts. For example, in lines 100-101: “The specimens used in the dry experiments (Figure 2a and 3) were sealed in plastic bags and stored in a freezer for 1-2 days before testing. The freezer temperature was set to -10°C.” can be replaced as: “The specimens used in the dry experiments (Figure 2a and 3) were sealed in plastic bags and stored in a freezer at -10°C for 1-2 days before testing.”

Re: Thanks for this constructive comment. We have modified the manuscript by removing some unnecessary parts.

15. Figure 4: Ice salinity shall be mentioned in the caption.

Re: Ice salinity is now provided in the caption of Figure 4.

Caption of Figure 4, “...thin sections of the ice (salinity: 5 ppt) ...”

16. Line 89: The verb “nucleated” fits better than “generated”.

Re: Thanks for pointing this out. Since this part of description is unnecessary, according to your Comment 14, we have deleted it.

## Referee #2

### Summary

This manuscript presents results from lab measurements and numerical models of the strain experience saline ice undergoing periodic compressive stress. The experimental set up is novel in that allows the ice sample to be immersed in water while stress is exerted by an electrohydraulic cylinder. This allows a vertical temperature profile to be maintained through the sample, which is more representative of sea ice conditions found outside the laboratory. The authors find measurable differences in the cumulative strain response between “wet” and “dry” experiments for all frequencies of periodic loading, which particularly significant differences at low frequencies. At a loading period of 1000s, the “dry” ice samples showed only 24% of the energy density dissipation as the “wet” samples. Using a dislocation-based model initially developed by co-author Cole and others, the authors are able to qualitatively and quantitatively reproduce the experimental results by assuming a significantly lower elastic modulus ( $E_0$ ), a higher dislocation density ( $\rho$ ), and a higher dislocation relaxation strength ( $\delta D^d$ ) for “wet” ice than “dry” ice.

Overall, the manuscript is well written the figures are clear and well labeled. The measured difference in strain response between “dry” and “wet” experiments suggests the non-isothermal temperature profile of immersed ice under a cold atmosphere has a significant effect on mechanical behavior, which should be considered in future experiments. However, I feel that some additional explanation is required regarding the methods used to determine the values of  $E_0$ ,  $\rho$  and  $\delta D^d$ . I believe the manuscript would also benefit from a deeper discussion of the temperature dependence of these and other parameters used in the model. My only other significant comment concerns the usage of the term “floating” in the manuscript. These comments are described in detail below, together with a list of minor comments for specific lines of text. In sum, I believe these amount to more than just minor revisions, but I feel they should all be quite straightforward to address.

**Re: We sincerely thank the reviewer for the encouragement on our work. The comments are constructive and insightful. We have modified our manuscript according to them.**

### Major Comments

#### 1. Unclear derivation of model parameters

The should provide the reader with more information about the empirical method used to determine the values for  $E_0$ ,  $\rho$  and  $\delta D^d$  listed in Table 4. Line 300 mentions a “trial and error” method, but it is not clear if applies just to  $E_0$  or other model parameters as well. Also, the text states on lines 295-296 that values for  $\delta D^{gb}$  were determined empirically, but these are not listed in Table 4 or mentioned elsewhere in the text. The authors should describe in detail the method used to determine the values for each parameter and provide an assessment of the sensitivity of the model to each parameter.

**Re: We thank the reviewer for the constructive comment. More information (as listed below) about the empirical method used to determine the values for  $E_0$ ,  $\rho$  and  $\delta D^{gb}$ , and an assessment of the sensitivity of the model to each parameter, have been added in the revised manuscript (as listed below). Please note that  $\delta D^d$  is dependent on  $\rho$  (Eq. (8)); once  $\rho$  is determined,  $\delta D^d$  is also known. Values for  $\delta D^{gb}$  could be found in Table 4.**

**Lines 271-279, “By making the slopes of the modeled and experimental hysteresis loops for  $T = 10$  s comparable,  $E_0$  could be determined. This is because the behavior of the specimens is mainly dominated by the un-relaxed modulus  $E_0$  when the loading frequency is high (here 0.1**

Hz to 1 Hz), as indicated in Figures 9 and 11. From Eqs. (9) and (10), one can find that the strain increment under one loading cycle is dependent on the dislocation density  $\rho$ ; based on this, the dislocation density  $\rho$  was estimated by using the experimental results of  $T = 100$  and  $500$  s and  $\delta D^d$  was then determined from Eq. (8).  $\delta D^{gb}$  was determined by referring to previous work (Cole 1995) because the grain boundary relaxation strength could be reasonably assumed constant for the ice material of interest here, and its effect on inelastic behavior of ice was significantly less than the dislocation mechanism”

Lines 383-386, “It was also found that for relatively high loading frequency (for example, 1 Hz used here), the modeled strain behavior was dominated by the un-relaxed modulus  $E_0$ , not sensitive to the dislocation density or the strength of grain boundary relaxation. However, for low-frequency (0.001 Hz) cyclic loading, the modeled specimen deformation was very sensitive to the dislocation density.”

## 2. Greater discussion of temperature dependence of mechanical behavior of saline ice

The difference in the observed strain response between wet and dry samples is attributed to the higher temperature of the wet ice, while the model results indicate that the difference is due to a lower elastic modulus,  $E_0$ , and higher dislocation density,  $\rho$ . However, the connection between these parameters and the temperature of the ice is not made clear. I recommend the authors expand their discussion to give the reader further insight into the temperature dependence of these two parameters. Also, the viscous strain rate,  $\dot{\epsilon}_v$ , is the only parameter specifically identified as having a temperature dependence (equation 10) and so I was surprised not to see greater discussion of this in the text.

Re: We thank the reviewer for the insightful comment. We have expanded our discussion to give readers further insight into the temperature dependence of  $E_0$  and  $\rho$ . Details can be found in the revised manuscript (as shown below).

Lines 392-396, “The analysis and modeling indicated that the physical mechanisms of deformation in both the warmer, floating specimens and the colder dry specimens were essentially the same. Warmer saline ice had a smaller modulus due to its higher liquid brine volume, which necessarily decreases the volume of the solid ice matrix (thereby reducing the bulk elastic modulus) and there is a pronounced increase in the effective  $\rho$  with increasing temperature (Cole and Durell, 2001; Timco and Weeks, 2010; Cole, 2020).”

## 3. Use of the phrase “floating ice”

I have two minor concerns with the use of the term “floating ice” in the manuscript:

a) First, I wonder whether the ice sample in the wet experiments can really be considered to be floating once the compressive stress is applied. If the water level were changed during the experiment, the sample would presumably not rise or fall. So, I wonder whether “immersed” would be a more appropriate term to use.

Re: Thanks for this comment. Before the ice specimen was compressed, it floated naturally on water. From the strain response of the ice, the change of water level can be determined to be in the magnitude of only 0.001 mm. Thus, it could be approximated that the specimen was still floating.

b) Second, in the discussion and conclusions section the phrase “floating ice” sometimes appears to be used to refer more generally to real world ice outside the laboratory. Specifically,

on line 373, the phrase is used almost synonymously with “full-scale”. I recommend that the authors add additional language to clarify that the “wet” lab experiments are able to replicate the temperature profile of floating ice, but not necessarily all the other ways in which the real world differs from the lab. See also specific comments below referring to lines 298 and 350.

Re: Thanks for the recommendation. Corresponding changes have been made in the revised manuscript (as shown below). More response can also be found below the related specific comments.

Lines 355-358, “Even if the use of floating specimens could be considered to only address the temperature profiles of in-situ floating ice (with some other environmental conditions of natural ice floes ignored)...”

#### Specific comments

Lines 51-52: This statement is not strictly accurate. One the air temperature rises above freezing in spring, the ice will approach an isothermal state

Re: Thanks for pointing this out. We have modified the statement in the revised manuscript.

Line 51, “Floating ice commonly has a through-thickness temperature gradient”

Line 83: It is not necessary or accurate to refer to the “bulk” salinity of seawater. The word “bulk” can be deleted.

Re: The corresponding change has been made in the revised manuscript. Thanks.

Line 106: Sea ice literature more commonly describes this microstructure as "non-oriented columnar".

For readers not familiar with the designators S2, S3, etc, I recommend the authors add some brief text explaining the relevant microstructures.

Re: Thanks for pointing this out. We have improved the text to avoid using the designators S1, S2 and S3.

Line 61, “non-oriented columnar saline ice specimens”

Line 93, “the columnar microstructure of the ice”

Line 256, “made of unaligned columnar ice”

Line 323, “non-oriented columnar ice”

Lines 206-207: This feature of the data could be highlighted with additional annotation. Also, the total amount of strain also seems to increase with loading period, with the exception of T=10s, which seems to yield less strain than T=1s or T=5s. Can the authors comment on this?

Re: Information on this is added to the revised manuscript.

Lines 177-180, “The total amount of strain does not strictly increase with the loading period. This may be because the loading platen and the specimen did not always achieve perfect contact immediately, causing some error in the strain measured in this initial stage of loading. Once intimate contact was achieved, the measured strain became reliable.”

Line 221: Mislplaced comma after “both”

Re: The sentence has been modified. Thanks.

Line 194, “both the strain increment per cycle and the area of one hysteresis loop”

Line 283: there should be a citation here for the value of  $\Omega$  for unaligned S2 saline ice.

Re: Thanks for pointing this out. The corresponding change has been made in the revised manuscript.

Line 256, “ $\Omega = 1/\pi \approx 0.32$  for a horizontal specimen made of unaligned columnar ice (Cole, 1995)”

Line 293: For clarity, I recommend adding “( $\rho$ )” after “dislocation density”

Re: The corresponding change has been made in the revised manuscript. Thanks.

Line 267, “the dislocation density ( $\rho$ )”

Line 298: Are the authors referring to field or lab measurements of floating ice here? Please also refer to general comment 1b above

Re: Originally, the statement was referring to field measurements of floating ice. Since more detailed information on how the parameter values were determined has now been provided, some redundant descriptions, including the sentence discussed in this comment, have been deleted from the revised manuscript.

Line 316: Should “modes” be “models”?

Re: Apologies for the typo. It has been corrected in the revised manuscript.

Line 350: A citation would be appropriate here. Additionally, it would be helpful to clarify whether the authors are referring to lab- or field-scale observations of the elastic modulus of floating ice (see also comment 1b above).

Re: Corresponding changes have been made in the revised manuscript.

Line 331, “...as would be expected based on full-scale observations on the effect of temperature on this property (Timco and Weeks 2010...)”

Lines 381-383: By using the phrase “the water and the related through-thickness temperature gradient”, the authors appear to suggest that water itself (and not just the resulting change in temperature profile) exerts some influence on the elastic modulus of the ice. Further clarification of this statement is needed.

Re: Thanks for pointing this out. We have modified the manuscript to make its main idea clearer by removing unnecessary and potentially misleading descriptions. The phrase mentioned here is deleted from the manuscript.



# 1 **Strain response and energy dissipation of floating saline ice** 2 **under cyclic compressive stress**

3 Mingdong Wei<sup>1</sup>, Arttu Polojärvi<sup>1</sup>, David M. Cole<sup>2</sup>, Malith Prasanna<sup>1</sup>

4 <sup>1</sup>Aalto University, School of Engineering, Department of Mechanical Engineering, P.O. Box 14100, FI-00076  
5 Aalto, Finland.

6 <sup>2</sup>ERDC-CRREL (Ret.), 72 Lyme Rd., Hanover, NH 03768, USA

7 *Correspondence to:* Arttu Polojärvi (arttu.polojarvi@aalto.fi)

8 **Abstract.** Understanding the mechanical behavior of sea ice is the basis of ice mechanics applications. Laboratory-  
9 scale work on saline ice has often involved dry, isothermal ice specimens due to the relative ease of testing. This  
10 approach does not address the fact that the natural sea ice is practically always floating in seawater and typically  
11 has a significant temperature gradient. To address this important issue, we have developed equipment and methods  
12 for conducting compressive loading experiments on floating laboratory-prepared saline ice specimens. The present  
13 effort describes these developments and presents the results of stress-controlled **sinusoidal** cyclic compression  
14 experiments. We conducted the experiments on dry, isothermal (-10°C) ice specimens and on floating ice  
15 specimens with a naturally occurring temperature gradient. The experiments involved ice salinities of 5 and 7 ppt,  
16 cyclic stress levels ranging from 0.04–0.12 MPa to 0.08–0.25 MPa and cyclic loading frequencies of **0.001** Hz to  
17 1 Hz. The constitutive response and energy dissipation under cyclic loading were successfully analyzed using an  
18 existing physically based constitutive model for sea ice. The results highlight the importance of testing warm and  
19 floating ice specimens and demonstrate that the experimental method proposed in this study provides a convenient  
20 and practical approach to perform laboratory experiments on floating ice.

## 21 **1 Introduction**

22 Climate change has led to an increased interest in polar sea areas and on ice behavior, since accurate predictions  
23 on the evolution of the ice conditions are crucial for modeling the future climate. Warming climate has also resulted  
24 in a search for more efficient marine transit routes, production of offshore wind power, industrial operations related  
25 to extraction of hydrocarbons, and even tourism in the north (Gagne et al., 2015; Serreze and Stroeve, 2015; Kern  
26 et al., 2019). Structural loads due to sea ice make these activities challenging. In-depth understanding of the  
27 physical and mechanical properties of sea ice is required to develop tools for modeling future ice conditions, the  
28 related ice–ice and ice–wave interaction problems, and for the design of safe and sustainable offshore structures

29 (Dempsey, 2000; Feltham, 2008, Herman et al., 2019a,b; Lu et al., 2018a,b; Ranta et al., 2017, 2018a,b; Tuhkuri  
30 and Polojärvi, 2018; Polojärvi et al., 2015; Voermans et al., 2019; Cheng et al., 2019; Li et al., 2015).

31 This paper studies the mechanical behavior of laboratory-prepared saline ice specimens under cyclic loading. This  
32 type of loading occurs in wave–ice and some ice–ice and ice–structure interaction problems – all important in the  
33 changing polar environment. For example, warming climate causes an increase in the amount of open water and  
34 broken ice fields, which strengthens the impact of waves on sea ice. From the perspective of pure ice mechanics  
35 and modeling of ice, the cyclic loading experiments yield information on the elastic and viscoelastic components  
36 of strain and their dependence on the physical, or microstructural, characteristics of the ice. The cyclic loading  
37 tests also give insight into the fatigue of ice (Haskell et al., 1996; Bond and Langhorne, 1997; Langhorne et al., 1998;  
38 Mellor and Cole, 1981; Murdza et al., 2019; Schulson and Paul, 2009; Iliescu et al., 2017; Iliescu and Schulson,  
39 2002).

40 Cyclic loading experiments on freshwater ice have been performed since the forties (Kartashkin, 1947; Mellor and  
41 Cole, 1981) and on saline ice since the eighties (Tabata and Nohguchi, 1980; Cole, 1995; Cole and Durell, 1995;  
42 Cole et al., 1998). Cole and Durell (1995) studied the effects of temperature (from -5 to -50°C), cyclic stress  
43 amplitude (from 0.1 to 0.8 MPa) and loading frequency (from 10<sup>-3</sup> to 1 Hz) on the response of laboratory-grown  
44 saline ice; the ice response was revealed sensitive to variations in these factors. Cole et al. (1998) investigated the  
45 response of columnar first-year sea ice to cyclic loading and found that the elastic, anelastic, and viscous strains  
46 varied according to the relation between the loading and preferred c-axis directions of the specimens. More recently,  
47 Heijkoop et al. (2018) conducted strain-controlled cyclic compression tests on sea ice to ascertain the variation of  
48 storage and loss compliances versus frequency. All of this earlier work has been performed using isothermal, dry  
49 specimens.

50 An often-overlooked issue in laboratory-scale experimentation is that most sea ice problems involve ice that is  
51 floating on water. Floating ice commonly has a through-thickness temperature gradient, resulting in a through-  
52 thickness gradient in its mechanical properties. The latter point is important to address in experimentation and  
53 modeling. The temperature gradient is implicitly taken into account in in-situ experiments on floating ice  
54 (Langhorne et al., 2015; Smith et al., 2015; Wongpan et al., 2018). The cost of in-situ experimental campaigns,  
55 however, is high and the experiments often require specially designed loading devices (Vincent and Dempsey,  
56 1999; Dempsey et al., 1999, 2018; Cole and Dempsey, 2004). Consequently, the relatively low costs and  
57 convenience of laboratory-scale work motivate the development of viable methods for laboratory-scale  
58 experiments on floating ice. Such experiments can be used, for example, for thorough validation of material models  
59 aiming to account for the temperature gradient in ice.

60 In the study presented here, stress-controlled sinusoidal cyclic compression experiments were performed on  
61 laboratory-grown, non-oriented columnar saline ice specimens floating on salt water and repeated on dry,  
62 isothermal (-10°C) specimens. The varied parameters were the ice salinity, cyclic stress amplitude and mean stress  
63 level, and the frequency of cyclic loading. The results are comprehensively analyzed and discussed, and are shown  
64 to compare favorably with the predictions of an existing physically-based constitutive model (Cole,1995).  
65 Techniques and observations yielding increased insight of the behavior of sea ice in its natural conditions are  
66 introduced; Insight on floating, rather warm, ice is important, as future sea ice is expected to be on average warmer  
67 than now (Boe et al., 2009; Blockley and Peterson, 2018; Ridley and Blockley, 2018).

68 The paper is organized as follows. Section 2 describes the specimen preparation, the experimental set-up, and the  
69 matrix of experimental variables. Section 3 presents the results from the experiments. Section 4 addresses  
70 constitutive modeling and Section 5 discusses our findings with references to earlier work and Section 6 gives our  
71 conclusions.

## 72 **2 Laboratory experiments of saline ice under cyclic loading**

### 73 **2.1 Saline ice specimen preparation and characterization**

74 The ice was grown in the cold room of Department of Mechanical Engineering, Aalto University using a tank  
75 having dimensions of 1.15 m × 1.15 m × 0.98 m (width × length × depth) and meltwater salinities of 24 and 34  
76 ppt. Rigid foam insulation was placed on the sides and bottom of the tank and heating cables were placed around  
77 the bottom perimeter to inhibit freezing from the structural members of the tank. Additionally, a hose for draining  
78 excess water was installed near the base of the tank, to prevent the accumulation of water pressure under the ice  
79 sheet during its growth. Such pressure could cause microcracking of ice or generate additional loads on the tank.  
80 Specimens having the nominal dimensions of 0.60 m × 0.30 m × 0.10 m were prepared by placing high-density  
81 polyethylene molds into the tank before seeding (Figure 1). The tolerance of the specimen dimensions was ±2 mm  
82 (in all stress calculations below, the measured dimensions of the specimens were used). The molds floated with  
83 2–3 mm of freeboard. Next, the saline water was chilled to about -1.5°C, the cold room temperature dropped to ≈  
84 -20°C and the tank was seeded by spraying very fine mist of fresh water over the tank as is typically done to seed  
85 ice sheets in larger-scale test basins (Gow, 1984; Li and Riska, 1996).  
86 After the seeding, the room temperature was increased to -14°C for three days and then -10°C for two days to  
87 produce the desired specimen thickness of 10 cm. The ice sheets made using 24 ppt and 34 ppt-saline water reached  
88 average salinities of 5 and 7 ppt, respectively, and their densities were  $886\pm 19$  and  $879\pm 16$  kg·m<sup>-3</sup>, respectively.

89 The specimens used in the dry experiments (Figure 2a and 3) were sealed in plastic bags and stored in a freezer at  
90  $-10^{\circ}\text{C}$  for 1–2 days before testing. However, for the floating ice experiments (see Figure 2b), the specimens were  
91 ejected from the molds, placed in plastic bags with water from the growth tank and quickly transferred to the test  
92 basin to minimize brine drainage during the transfer.

93 Before the experiments, the columnar microstructure of the ice was verified by producing and inspecting thin  
94 sections as detailed by Langway (1958). Of special interest was the microstructure close to the specimen  
95 boundaries since such molds are somewhat uncommon in ice specimen preparation. Figure 4 shows two typical  
96 thin sections from near the boundary of a specimen produced using 34-ppt-saline water; one is for the vertical and  
97 the other for the horizontal direction as indicated. Figure 4a shows the columnar structure of the ice. The horizontal  
98 view in Figure 4b provides a way to estimate the average grain size by dividing the section area by the number of  
99 grains; the average grain size was  $\approx 3.5$  mm. The Schmidt equal area net pole projection for one of the thin sections  
100 shown in Figure 5 confirms that the c-axes were unaligned in the horizontal plane, as intended.

101

## 102 2.2 Equipment, test matrix and experimental procedure

103 The experiments were conducted in the same cold chamber used for the saline ice production. As Figures 2 and 3  
104 illustrate, an externally mounted electrohydraulic cylinder applied loads to the specimens. The piston passed  
105 through a sealed port in the side of the test tank. The piston had a maximum stroke of 800 mm and a loading  
106 capacity of 100 kN for compression and 60 kN for tension. The load cell had an accuracy of  $\pm 5$  N, which is  
107 sufficient for all stress levels and cycles of the experiments here. The test basin was constructed of waterproof  
108 plywood. The system employed a camera for remote monitoring of the experiments, a three-channel temperature  
109 datalogger to record the temperature profile of floating ice during testing, a Data Acquisition Processor (DAP)  
110 board (model: Data Translation DT9834), and fixtures for arranging displacement sensors to the ice specimens.  
111 The temperature datalogger had a maximum sampling rate of one datum per five seconds, its measurement range  
112 was from  $-100$  to  $1300^{\circ}\text{C}$ , and an accuracy of  $\pm 0.5^{\circ}\text{C}$ . The DAP board could achieve a maximum scan rate of  
113 500,000 samples per second.

114 The loading system has a self-equilibrating geometry in that the compressive force applied by the electrohydraulic  
115 piston and transmitted through the specimen is balanced by a tensile force in the external load frame (Figure 3).  
116 Care was taken to center the loading piston and the reaction plates on the vertical dimension of the load frame.

117 The ice deformation was measured as follows. Before the test, two holes were drilled on the specimen. Two iron  
118 rods with the cross-section of  $5\text{ mm} \times 5\text{ mm}$  were then inserted into the holes and frozen in place using a small  
119 quantity of cold fresh water. The relative displacement of the rods was monitored by two linear variable differential

120 transformer transducers (LVDTs, model: HBM WA2, with a measurement range and accuracy of 2 and  $\pm 0.001$   
121 mm, respectively). This relative displacement was used to determine the strain response of the specimen. As shown  
122 in Figures 2 and 3, the LVDTs were mounted on a rectangular steel placed across the basin.

123 The air temperature was kept at  $-10^{\circ}\text{C}$  during all testing. To measure the through-thickness temperature gradient  
124 in all of the floating ice experiments, temperature probes were frozen into three 2.5 mm-diameter, 50 mm deep  
125 holes were drilled on one side face of the specimen. As shown in a sketch of Figure 6a, one measurement point  
126 was in the middle of the specimen from the vertical direction, and the other two were 1.5 mm away from the upper  
127 and lower surfaces of the specimen, respectively. During each floating ice experiment, temperature readings from  
128 all three channels remained constant for the duration of the experiment, indicating that the thermal gradient was  
129 unaffected by the cyclic loading.

130 Figure 6b presents typical temperature profiles measured in two floating ice specimens. For the 5-ppt-saline  
131 floating ice, the temperature near the top surface, in the middle and near the bottom surface of the specimen was  
132 measured to be  $-3.0$ ,  $-2.3$  and  $-2.2^{\circ}\text{C}$ , respectively, while the values were  $-3.1$ ,  $-2.4$  and  $-2.1^{\circ}\text{C}$ , respectively, for  
133 the 7-ppt-saline ice floe. These temperature readings suggest that the average temperature of the floating ice was  
134  $-2.5^{\circ}\text{C}$ , much higher than the air temperature of the cold chamber ( $-10^{\circ}\text{C}$ ). The water temperature at five  
135 centimeters below the water surface was measured to be  $\approx -1.8^{\circ}\text{C}$  in the floating ice tests.

136 The test matrix called for applying relatively low cyclic compressive stress levels with the system in load control.  
137 Figure 7 presents the loading waveforms used in the experiments and the test matrix is given in Table 1. In the  
138 experiments, the ice was first loaded with a linear ramp to reach an initial compressive stress level, at which point  
139 a compressive haversine waveform was immediately applied. In Figure 7a,  $\sigma_{\max}$  and  $\sigma_{\min}$  represent the upper and  
140 the lower bounds of the cyclic compressive stress, respectively, and  $T$  denotes the period for one loading cycle. As  
141 indicated by Table 1, six periods ranging from 1 to  $10^3$  s were employed; these periods cover the main range of  
142 ocean wave periods, which usually vary from several seconds to tens of seconds (Reistad et al., 2011; Zijlema et  
143 al., 2012). In each dry test, only a fixed frequency was applied. Once the test was completed, the specimen  
144 recovered for 15 minutes before subsequent load cycles were applied. For all dry tests, the duration of the initial  
145 loading ramp was fixed to be 1 s. In each of the tests corresponding to  $T = 1, 5, 10$  and  $100$  s, 18 cycles were  
146 applied ( $N = 18$ ), while for those with  $T = 500$  and  $1000$  s,  $N = 9$  and  $4$ , respectively. The sequence of loading  
147 cycles was in ascending order of  $T$  in all cases. As a time-saving measure, and to avoid freezing of the open water  
148 in the basin, cyclic stresses with increasing periods were applied continuously in the floating ice tests. The number  
149 of cycles for each period was as follows:  $T = 1, 5$  or  $10$  s,  $N = 10$ , for  $T = 100$  s,  $N = 2$ , and for  $T = 500$  or  $1000$  s,  
150  $N = 1$ .

151 The cyclic compressive stress applied to the dry specimens varied from 0.08 to 0.25 MPa, which could be  
152 justifiably expected to not lead to severe damage of the specimen while being high enough to generate measurable  
153 strain (Cole and Dempsey, 2001). The stress in the floating experiments was lower, varying from 0.04 to 0.12 MPa,  
154 to avoid damage. For each case listed in Table 1, two specimens harvested from two ice sheets were subjected to  
155 each set of conditions. The specimens were named according to their salinity, test conditions (dry/floating), and  
156 the ice sheet from which it originated. For example, specimen name Dry-5ppt-1 indicates that it came from the  
157 first 5-ppt-saline ice sheet and was tested under the dry, isothermal conditions.

158 Figure 7b illustrates how the energy dissipation in the cyclic loading experiments was calculated. For common  
159 engineering materials subjected to uniaxial cyclic compression, the strain along the compressive direction versus  
160 the stress is usually characterized by hysteresis loops. The strain energy density dissipated in a loading cycle can  
161 be determined by integrating the stress-strain curve. As shown in Figure 7b, the area under the loading curve  
162 (region ABCF) represents the maximum strain energy input via the testing machine during a load cycle, and the  
163 area under region CDEF denotes the strain energy released during the unloading portion of the cycle. The energy  
164 density dissipation (EDD) in one full loading-unloading cycle is given by the difference between the areas of  
165 regions ABCF and CDEF (Liu et al., 2017, 2018). The energy density consumed in the hysteresis loop can, in  
166 general, be attributed to the internal friction and, in some cases, damage to the material. For each cycle, the energy  
167 dissipation rate (EDR) can be defined as the ratio of the dissipated energy to the input energy, namely the area of  
168 the region ABCDE divided by that of the region ABCF.

### 169 3 Experimental results

170 Figure 8 presents strain-time plots obtained from the dry experiments using specimen Dry-5ppt-1 under the  
171 indicated conditions. The strain-time curves manifest the following feature: If a line would be drawn through the  
172 maximum value for each cycle, the slope of the line would first decrease from its initial value for some number of  
173 cycles and then settle down to an almost constant value. This observation means that the strain response of the ice  
174 specimen under sinusoidal compressive stress reaches a relatively steady stage after the initial transient of the  
175 anelastic strain is exhausted, and that in this steady stage the accumulated viscous or permanent strain increases  
176 linearly with time. In addition, Figure 8 shows that the longer the period  $T$  of cyclic loading, the larger the strain  
177 amplitude in one steady-stage cycle. The total amount of strain does not strictly increase with the loading period.  
178 This may be because the loading platen and the specimen did not always achieve perfect contact immediately,

179 causing some error in the strain measured in this initial stage of loading. Once intimate contact was achieved, the  
180 measured strain became reliable.

181 Figure 9 shows the stress-strain curves for the same experiments. In each case, the area of the hysteresis loop for  
182 the first few cycles was comparatively large, and then gradually decreased to a constant value as the specimen  
183 reached the steady deformation stage described in the previous paragraph. For example, the hysteresis loops after  
184 the first stress cycle in the dry experiment with  $T = 1000$  s are similar;  $N = 4$  is enough for the dry specimen at  $T$   
185 = 1000 s to show steady-state response. Thus, the EDD (Figure 7b) decreases from its initial value to an  
186 approximately constant value. It is clear that the steady-state hysteresis loop area increase with the period of the  
187 cyclic loading, consistent with earlier studies (Cole, 1990; Murdza et al., 2018; Weber and Nixon, 1996).

188 Figures 10 and 11 display a set of strain-time plots and the corresponding stress-strain curves for the floating ice  
189 experiments on the 5-ppt-saline ice specimens, respectively. The curves in these two figures show similar features  
190 to those in Figures 8 and 9 for dry experiments: The floating ice also reached a steady state of deformation after  
191 some loading cycles and the amplitude of the steady-state strain response still increased with  $T$ . Similar to the  
192 results of the dry experiments, Figure 11 indicates that the longer the loading period, the larger the strain increment  
193 of the floating specimen under one steady-state loading-unloading cycle. Comparison of Figures 9 and 11 in the  
194 steady state shows that, for constant  $T$ , both the strain increment per cycle and the area of one hysteresis loop, are  
195 larger in the floating ice experiments than in the dry experiments even though the stress levels are lower than in  
196 the dry experiments. It is thus evident that the decreased stress levels in the floating ice experiments did not fully  
197 compensate for the temperature effects on the viscous and viscoelastic components of strain as, for example, the  
198 viscous strain rate of floating 5-ppt-saline ice specimen is fourteen times that of the corresponding dry specimen.

199 The energy density dissipation (EDD) and the energy dissipation rate (EDR) per cycle during steady-stage  
200 deformation (Section 2.2 and Figure 7b) allow quantitative comparisons of the inelastic behavior of specimens as  
201 a function of test conditions. These are presented in Tables 2 and 3 for all, except the 1-second-period, experiments,  
202 for which the hysteresis loop areas are too small for accurate measurements. Tables 2 and 3 indicate that both the  
203 EDD and the EDR decrease with the increase of loading frequency. Moreover, under the same frequency, the 7-  
204 ppt-saline ice has larger EDD and EDR values than the 5-ppt-saline ice irrespective of the experiment type. In  
205 addition, the floating ice experiments always exhibit higher EDD and EDR values than the dry experiments  
206 regardless of the ice salinities. The differences in the values of EDD are especially significant for low frequencies.  
207 For example, in the experiments with  $T = 1000$  s, the average value of EDD for the 5-ppt-saline dry specimens is  
208 only 24% of that of the 5-ppt-saline floating specimens and 44% of that of the 7-ppt-saline dry specimens. However,  
209 for the experiments with  $T = 5$  s, the average value of EDD in the former case is 47% and 77% of that in the latter

210 two cases, respectively. Thus, the ice salinity and **the test conditions** have a more significant influence on the  
211 energy dissipation of the ice when the cyclic loading period is long.

## 212 **4 Material modeling**

213 The hysteresis loops of the stress-strain curves manifest viscous and anelastic properties of the ice. According to  
214 previous studies (Cole, 1995; Leclair et al., 1999), in low-stress cyclic loading experiments, the microstructure of  
215 the ice remains unaffected by loading, or in other words, no damage occurs within the material. In the present case  
216 of polycrystalline ice, the anelastic deformation is mainly attributed to two relaxation mechanisms, lattice  
217 dislocation relaxation and grain-boundary sliding. Viscous straining is attributable to basal dislocation glide. In  
218 this section, a dislocation-based model (Cole, 1995; Cole and Durell, 2001), which accounts for these mechanisms,  
219 is used to predict the strain response of the ice specimens based on their physical properties and experimental  
220 conditions. Here the model is only briefly described, but a detailed description can be found from Cole et al. (1998),  
221 where the model is also demonstrated to reproduce the viscous and anelastic behavior of dry specimens. Here the  
222 applicability of the model in predicting the behavior of floating laboratory-prepared ice specimens subjected to  
223 cyclic loading is tested for the first time.

224

### 225 **4.1 Brief description of the model**

226 In the physically based model by Cole (1995) and Cole and Durell (2001), the axial strain,  $\varepsilon$ , of ice under uniaxial  
227 cyclic compression is considered to be composed of elastic, anelastic (delayed elastic) and viscous components,  
228 denoted here as  $\varepsilon_e$ ,  $\varepsilon_a$  and  $\varepsilon_v$ , respectively. The axial strain is expressed as

$$229 \quad \varepsilon = \varepsilon_e + \varepsilon_a + \varepsilon_v. \quad (1)$$

230 In the case of sinusoidal stress waveform,  $\varepsilon_e$  can be written as

$$231 \quad \varepsilon_e = \frac{\sigma(\omega, t)}{E_0}, \quad (2)$$

232 where  $\omega$  is the angular frequency of the stress waveform and  $E_0$  is the unrelaxed modulus. Although detailed  
233 expressions have been developed for the effective elastic modulus as a function of crystallography, brine and gas  
234 porosity, and temperature, a simplified approach is adopted in the present effort. The anelastic component  $\varepsilon_a$   
235 incorporates both above-mentioned relaxation mechanisms to represent the time-dependent recoverable  
236 deformation. For the steady-stage deformation,  $\varepsilon_a$  of ice subjected to sinusoidal compressive stress can be  
237 decomposed as (Cole and Dempsey 2001)

$$238 \quad \varepsilon_a = \sigma(\omega, t) \left[ D_1^d(\omega) + D_2^d(\omega) + D_1^{gb}(\omega) + D_2^{gb}(\omega) \right], \quad (3)$$



239 where the compliance terms,  $D$ , with the superscripts “d” and “gb” denote the compliances induced by dislocation  
 240 and grain boundary sliding, respectively. The compliance terms are defined as (Cole et al., 1998)

$$241 \quad D_1^d(\omega) = \delta D^d \left\{ 1 - \frac{2}{\pi} \tan^{-1} \left[ e^{(\alpha^d S^d)} \right] \right\} \quad (4)$$

$$242 \quad D_1^{gb}(\omega) = \delta D^{gb} \left\{ 1 - \frac{2}{\pi} \tan^{-1} \left[ e^{(\alpha^{gb} S^{gb})} \right] \right\} \quad (5)$$

$$243 \quad D_2^d(\omega) = \alpha^d \cdot \delta D^d \frac{1}{e^{(\alpha^d S^d)} + e^{(-\alpha^d S^d)}} \quad (6)$$

$$244 \quad D_2^{gb}(\omega) = \alpha^{gb} \cdot \delta D^{gb} \frac{1}{e^{(\alpha^{gb} S^{gb})} + e^{(-\alpha^{gb} S^{gb})}}, \quad (7)$$

245 where  $S^d = \ln(\tau^d \omega)$ ;  $\tau^d$  is the central relaxation time (Cole and Durell, 1995).  $\alpha$  is a so-called peak broadening  
 246 term, which accounts for the effect of a distribution in relaxation times of the basal plane dislocations. The grain  
 247 boundary relaxation is calculated using similar mathematic expressions as the dislocation relaxation, but has a  
 248 different strength, activation energy and peak-broadening term. The activation energy is 1.32 eV for the grain  
 249 boundary relaxation and 0.55 eV for the dislocation relaxation (Cole and Dempsey, 2001). The peak-broadening  
 250 terms for lattice dislocation relaxation and grain-boundary sliding relaxation are typically  $\approx 0.5$  and 0.6,  
 251 respectively, determined experimentally by Cole (1995), Cole and Dempsey (2001) and also validated by Heijkoop  
 252 et al. (2018). The strength of the dislocation relaxation is calculated from

$$253 \quad \delta D^d = \frac{\rho \Omega b^2}{K}, \quad (8)$$

254 where  $b$  represents Burgers vector ( $b = 4.52 \times 10^{-10}$  m);  $\rho$  denotes the mobile dislocation density, often found to  
 255 be on the order of  $10^9$  m<sup>-2</sup>;  $\Omega$  is an orientation factor, determining the average basal plane shear stress induced by  
 256 the background normal stress ( $\Omega = 1/\pi \approx 0.32$  for a horizontal specimen made of **unaligned columnar** ice (Cole,  
 257 **1995**));  $K$  is a restoring stress constant, determined as 0.07 kPa for polycrystalline ice in experiments (Cole and  
 258 Durell 2001).

259 In Eq. (1), the viscous strain  $\varepsilon_v$  is often estimated with the following formulae (Cole and Durell, 2001):

$$260 \quad \varepsilon_v = \int_0^t \dot{\varepsilon}_v d\bar{t} \quad (9)$$

$$261 \quad \dot{\varepsilon}_v = \frac{\beta \rho \Omega^{1.5} b^2 \sigma_{\text{creep}}}{B_0} e^{\left( \frac{Q_{\text{glide}}}{kT} \right)}, \quad (10)$$

262 where  $\beta = 0.3$ ,  $Q_{\text{glide}} = 0.55$  eV, and  $B_0 = 1.205 \times 10^{-9}$  Pa·s.  $k$  is Boltzmann's constant,  $T^*$  is the temperature in  
263 Kelvins. By using the above definitions and equations, the strain of the ice specimen can be finally determined via  
264 Eq. (1).

265

## 266 4.2 Modeling

267 In this study, the key quantity to be determined from the experiments is the dislocation density ( $\rho$ ). With knowledge  
268 of the microstructure and orientation factor ( $\Omega$ ), and given the experimental conditions, the anelastic term  $\delta D^d$  and  
269 the viscous strain rate can be calculated directly. We opt here to determine  $E_0$  empirically. These were done by  
270 trial and error until the stress-strain curves generated by the model matched with those measured in the experiments  
271 with  $T = 10, 100$  and  $500$  s. **By making the slopes of the modeled and experimental hysteresis loops for  $T = 10$  s  
272 comparable,  $E_0$  could be determined. This is because the behavior of the specimens is mainly dominated by the  
273 un-relaxed modulus  $E_0$  when the loading frequency is high (here 0.1 Hz to 1 Hz), as indicated in Figures 9 and 11.  
274 From Eqs. (9) and (10), one can find that the strain increment under one loading cycle is dependent on the  
275 dislocation density  $\rho$ ; based on this, the dislocation density  $\rho$  was estimated by using the experimental results of  
276  $T = 100$  and  $500$  s and  $\delta D^d$  was then determined from Eq. (8).  $\delta D^{\text{gb}}$  was determined by referring to previous work  
277 (Cole 1995) because the grain boundary relaxation strength could be reasonably assumed constant for the ice  
278 material of interest here, and its effect on inelastic behavior of ice was significantly less than the dislocation  
279 mechanism. The values determined for the parameters are tabulated in Table 4. Subsequently, the model based on  
280 these parameter values was applied to predict the test results for other loading periods. An example of the  
281 comparison of experimental and modeling results is presented in Figure 12, in which the steady-state strain curves  
282 from all dry experiments on the 5-ppt-saline ice specimen are accompanied by the simulated ones.**

283 Figure 12 shows that the modeled strain records compare well with those from the experiments with period  $T = 1,$   
284  $5$  and  $1000$  s. The model reproduced the steady-state strain response of the specimens very well for all tested  
285 frequencies. Figure 13 presents the stress-strain hysteresis loops from the same experiments together with those  
286 produced by the model. The hysteresis loops generated by using the model are very similar to those from the  
287 experiments. The loop area increases with  $T$  in both the experiments and simulations.

288 For assessing the model in more detail, the values of EDD and EDR derived using it are given in Tables 5 and 6,  
289 respectively, and moreover, compared with the data from all the experiments (the test matrix is given in Table 1).  
290 Tables 5 and 6 indicate that the model predicts well the values of EDD and EDR for all cyclic loading periods  
291 studied here. In general, the error in the predicted EDD and EDR values are within 20%, with the exception of  
292 only few cases. No obvious trend between the magnitude of error and loading period or experiment type was

293 observed. Note that for a given ice specimen, one dislocation density value adequately models the steady-state  
294 strain responses and energy dissipation values in tests conducted with different frequencies. The value of  
295 dislocation density, thus, remained constant through the cyclic loading.  
296

### 297 **4.3 Further validation**

298 The above results show that the model can yield satisfactory predictions on the viscous and anelastic behavior of  
299 both dry and **floating** specimens. One may argue that the good agreement between the model predictions and the  
300 experimental results only indicates the capability of the model to predict the results for the experiments with the  
301 same stress levels as those used to calibrate the model parameters. To check whether the model can predict the  
302 results of the experiments with different stress levels than those above, additional experiments were performed on  
303 specimen Dry-5ppt-1 with higher stress (0.1–0.3 MPa) and on specimen **Floating-7ppt-1** with lower stress (0.005–  
304 0.085 MPa) (**Nominal cyclic stress of 0.005–0.085 MPa is low, but the setup could achieve it: With the accuracy**  
305 **of the system, the actual stress applied to the specimen was 0.005 ( $\pm 0.001$ )–0.085 ( $\pm 0.003$ ) MPa**). The model was  
306 then used to **determine** the strain response and energy dissipation in these tests using the parameterization based  
307 on the experiments of Section 3 (Table 4).

308 Figure 14 compares the stress-strain hysteresis loops obtained in the supplementary experiments with the  
309 predictions yielded from the model. Good agreement is observed between the predicted and measured hysteresis  
310 loops. Again, the relative errors in the EDD and EDR values are found to be less than 20% for **most** data sets. The  
311 model is, indeed, capable of predicting the deformation of saline ice in a dry environment or when floating in water  
312 irrespective of the stress level (given that the stress levels are moderate and do not cause an increase in dislocation  
313 density during deformation). The applicability of the model is highlighted by the fact that once the model  
314 parameters are calibrated through benchmark experiments (**the elastic modulus and dislocation density in the**  
315 **present case**), it yields sound predictions for the experiments conducted with other stress levels.

### 316 **5 Discussion**

317 Although past laboratory-scale work has provided insight into the mechanical behavior of sea ice, the work has  
318 been mostly performed using relatively cold, dry and isothermal specimens. The results above indicate that more  
319 attention should be paid to the mechanical behavior of relatively warm, floating ice **with a naturally occurring**  
320 **temperature gradient**. Here efforts were made to develop a relatively low-cost, convenient and useful approach for  
321 laboratory-scale floating ice experiments and for preparing small-scale, saline columnar ice specimens. The thin  
322 sections (Figures 4 and 5) indicated that the measures taken on the ice production guaranteed the generation of

323 non-oriented columnar ice. Moreover, the thin sections showed that the molds used for specimen preparation do  
324 not influence the columnar ice microstructure. This is encouraging, as molds are not often incorporated into  
325 growing sheets of non-oriented columnar ice. The use of molds in this way significantly simplified specimen  
326 preparation and resulted in accurate dimensions. The molds are especially effective in the experiments on floating  
327 ice specimens: The specimens thus produced have proper dimensions, require no cutting, have a realistic  
328 temperature gradient and can be quickly transferred to the test basin, so brine loss is minimized.

329 The results above are in qualitative agreement with what would be expected for floating ice, as for example,  
330 floating specimens having through thickness thermal gradient and mean temperature of  $-2.5^{\circ}\text{C}$  exhibit lower  
331 modulus and more pronounced inelastic deformation in comparison with dry specimens at  $-10^{\circ}\text{C}$ , as would be  
332 expected based on full-scale observations on the effect of temperature on this property (Timco and Weeks 2010;  
333 Cole 2020). This gives confidence on the methods employed in the production and mechanical testing of the  
334 specimens. Further, the good agreement between the results for floating ice and the corresponding model  
335 predictions show quantitative validity of the approach taken here. All-in-all, the results suggest that the chosen  
336 experimental techniques (including the loading system, the strain measurement scheme, the data acquisition  
337 system and settings) worked well and provided useful results for the analysis. An exception is some of the 1-  
338 second-period experiments, which yielded strain responses with unexpected features; this is because the hysteresis  
339 loop areas are very small in size, making accurate measurements with the used set-up challenging. This could be  
340 circumvented in the future experiments by using techniques and devices with even higher precision and setting a  
341 higher sampling rate of data acquisition. The methods proposed in this study to conduct laboratory experiments  
342 on floating ice experiments are practical and can provide a convenient approach for relatively low-cost  
343 experimentation on floating ice.

344 The laboratory work here not only demonstrated the availability of the proposed experimental methods, but also  
345 contributes to the understanding of the constitutive behavior of ice. A common trend in developing material models  
346 is to ensure they have a solid physical basis, that is, that they are based on an understanding of the physical  
347 processes that underlie the mechanical phenomena of interest. Above we used one such physically-based model  
348 introduced by Cole (1995). Earlier work, which has been based on the experiments resembling the dry experiments  
349 here, has shown that the model is capable of predicting the inelastic deformation of sea ice via dislocation-based  
350 mechanisms and is able to estimate the effective dislocation density in ice from experimental results. Here the  
351 model was successfully validated against the results from the floating ice experiments. Moreover, the results  
352 indicated that once the constant dislocation density value of the specimens was determined, the model adequately  
353 predicted the steady-stage deformation for the cyclic loading experiments conducted with different frequencies

354 and stress levels. Even if the use of floating specimens could be considered to only address the temperature profiles  
355 of in-situ floating ice (with some other environmental conditions of natural ice floes ignored), the above results  
356 bring confidence to the model and demonstrate its potential in modeling practical applications involving ice in  
357 such conditions, especially considering that some research has been launched to devote to a numerical  
358 implementation of the model (O'Connor et al., 2020).

359 The good agreement between the experimental and modeling results also motivates discussion on the parameter  
360 values in Table 4. Expectedly, the floating ice specimens have lower unrelaxed moduli than the dry specimen. For  
361 the 5-ppt and 7-ppt-saline ice, the average elastic modulus of the floating specimens is 66% and 55% lower than  
362 that of the dry specimens, respectively. In the dry experiments, the isothermal 7-ppt-saline ice has a 31% lower  
363 average elastic modulus than the 5-ppt-saline ice. In the floating ice experiments, the 7-ppt-saline specimen still  
364 has a lower average elastic modulus than the 5-ppt-saline specimen, but the difference, 8%, is not as prominent as  
365 in the dry experiments. Thus, the fact that the ice was in contact with water and had a realistic temperature profile  
366 had a larger influence on the elastic modulus of ice than the variation of the ice salinities studied here.

367 Table 4 also indicates that the dislocation densities determined for the ice specimens were on the order of  $\sim 10^8$ –  
368  $10^{10} \text{ m}^{-2}$ , and thus were in good agreement with values in the  $10^9 \text{ m}^{-2}$  order of magnitude given by Cole (1995).  
369 Moreover, the dislocation density of the floating ice was approximately one order of magnitude greater than that  
370 of the dry specimen. Note that there is precedent showing the dislocation density of ice increasing with temperature  
371 (Cole and Durell, 2001; Cole, 2020). The same trend is seen here when the experiments change from dry specimens  
372 ( $-10^\circ\text{C}$ ) to relatively warm, floating, ones. In addition, the earlier work cited has shown that the dislocation density  
373 increases with the salinity. Therefore, the calculated dislocation densities make sense physically and are generally  
374 in line with expectations.

375 Specimens originating from two different ice sheets were tested. Table 4 shows that for a given set of conditions,  
376 the elastic modulus of the specimens showed only small variations from one sheet to another. Compared with the  
377 elastic modulus, the relative change in dislocation density was fairly large, which may be due to heterogeneity of  
378 ice. A similar degree of change in dislocation density was also reported by Cole and Durell (2001) related to dry,  
379 isothermal, ice specimens. As for the strength of the grain boundary relaxation, its value was taken as  $2 (\pm 1) \times 10^7$   
380  $\text{Pa}^{-1}$  for all specimens since variations in grain size among the ice specimens was small. Thus, here the main  
381 quantity to be determined from the experimental results for studying anelastic strain response of the specimens  
382 was the dislocation density. It was also found that for relatively high loading frequency (for example, 1 Hz used  
383 here), the modeled strain behavior was dominated by the un-relaxed modulus  $E_0$ , not sensitive to the dislocation

384 density or the strength of grain boundary relaxation. However, for low-frequency (0.001 Hz) cyclic loading, the  
385 modeled specimen deformation was very sensitive to the dislocation density.

386 The effect of water on the mechanical behavior of floating ice has also been attributed on temperature (Golden et  
387 al., 2007). Moreover, the specimens harvested from floating ice sheets lose brine once removed from the sheet;  
388 warm ice in particular can lose a significant amount of brine which could significantly alter the mechanical  
389 properties in subsequent experiments. In addition, some remaining brine (for example, some of those in capillary  
390 brine channels) must freeze during the storage process of dry specimens; this may as well lead to some difference  
391 in the macroscopic mechanical behavior (for example, in elastic modulus) of dry and floating specimens  
392 (Marchenko and Lishman, 2017; Eicken, 1992; Jones et al., 2012; Gough et al., 2012). The methodology developed  
393 in the present effort avoids such problems and is expected to produce more realistic mechanical behavior,  
394 particularly when interest centers on behavior at relatively warm temperatures where brine drainage is extensive.  
395 The analysis and modeling indicated that the physical mechanisms of deformation in both the warmer, floating  
396 specimens and the colder dry specimens were essentially the same. Warmer saline ice had a smaller modulus due  
397 to its higher liquid brine volume, which necessarily decreases the volume of the solid ice matrix (thereby reducing  
398 the bulk elastic modulus) and there is a pronounced increase in the effective  $\rho$  with increasing temperature (Cole  
399 and Durell, 2001; Timco and Weeks, 2010; Cole, 2020).

## 400 **6 Conclusions**

401 Equipment and methods were developed to conduct laboratory experiments to examine the mechanical properties  
402 of floating saline ice specimens with a naturally occurring temperature gradient. In this initial effort, we examined  
403 the strain response of floating saline ice under cyclic compressive stresses and conducted reference experiments  
404 under dry, isothermal conditions. The experiments examined specimens having one of two nominal salinities (5  
405 and 7 ppt), cyclic loading frequencies from  $10^{-3}$  to 1 Hz were applied and two levels of cyclic stress were applied.  
406 The experimental results compared favorably with the theoretical predictions obtained using a physically based  
407 constitutive model for saline ice. Given the limitations of the experiments program, the following conclusions can  
408 be drawn.

409 **Equipment and methods:**

- 410 1. Groups of unaligned, columnar grained saline ice specimens can be produced simultaneously in the  
411 laboratory using floating molds, and the presence of the molds has no observable effect on their  
412 microstructure.

413 2. The use of molds produced specimens that could be placed directly in the mechanical testing fixture, which  
414 for the case of floating ice experiments, provided a way to maintain a realistic temperature gradient during  
415 subsequent experimentation.

416 3. The experimental apparatus, which employed an electrohydraulic actuator and a saline water tank placed  
417 in a cold room, provided a way to apply in-plane loads to floating ice specimens and successfully produced  
418 monotonic and cyclic loading waveforms employed in more conventional systems.

419 **Constitutive modeling:**

420 4. The dislocation mechanics of the model employed in the analysis can reproduce well the strain response  
421 and energy dissipation of saline ice subjected to cyclic loading for floating ice or dry specimens, and for the  
422 observed ice salinities. The results show that the prediction errors of the energy density dissipation and the  
423 energy release rate are within  $\approx 20\%$ .

424 5. For either dry or **floating** specimens, the higher the salinity of ice, the lower the modulus ( $E_0$ ) and the larger  
425 the dislocation density ( $\rho$ ). In addition,  $E_0$  is much higher and  $\rho$  is far smaller for the dry specimens than for  
426 the **floating** specimens, provided other experimental variables are consistent.

427 **This work makes it clear that the mechanical behavior of floating specimens of saline ice can be examined in the**  
428 **laboratory under a reasonable approximation of in-situ conditions and with good efficiency. This capability opens**  
429 **the door to more sophisticated experimental work on saline ice under more realistic environmental conditions than**  
430 **previously possible.**

431 **Financial support:** The authors are grateful for the financial support from the Academy of Finland through the  
432 project (309830) Ice Block Breakage: Experiments and Simulations (ICEBES).

433 **Acknowledgments:** The authors thank the help from the technical staff of Aalto University Department of  
434 Mechanical Engineering, and especially, from Kari Kantola and Veijo Laukkanen.

435 **Author contributions:** AP, MW and DMC designed the study. MW and MP performed the experiments. MW,  
436 AP and DMC contributed to the interpretation of the results. MW, AP and DMC drafted the paper. All authors  
437 commented on the text.

438 **Code and data availability:** The code used for material modeling is written in MATLAB. Scripts used for analysis  
439 and more detailed information of the experimental results are available from the authors upon request.

440 **Competing interests:** The authors declare that they have no conflict of interest.

#### 441 **References**

442 Blockley, E. W. and Peterson, K. A.: Improving Met Office seasonal predictions of Arctic sea ice using assimilation  
443 of CryoSat-2 thickness, *The Cryosphere*, 12, 3419–3438, <https://doi.org/10.5194/tc-12-3419-2018>, 2018.

444 Boe, J. L., Hall, A., and Qu X.: September sea-ice cover in the Arctic Ocean projected to vanish by 2100, *Nat.*  
445 *Geosci.*, 2, 341–343, doi:10.1038/ngeo467, 2009.

446 **Bond, P. E. and Langhorne, P. J.: Fatigue behavior of cantilever beams of saline ice, *J. Cold Reg. Eng.*, 11, 99–**  
447 **112, [https://doi.org/10.1061/\(ASCE\)0887-381X\(1997\)11:2\(99\)](https://doi.org/10.1061/(ASCE)0887-381X(1997)11:2(99)), 1997.**

448 Cheng, S., Tsarau, A., Evers, K. U., and Shen, H.: Floe size effect on gravity wave propagation through ice covers,  
449 *J. Geophys. Res.-Oceans*, 124, 320–334, <https://doi.org/10.1029/2018JC014094>, 2019.

450 **Cole, D. M.: Reversed direct-stress testing of ice: Initial experimental results and analysis. *Cold Reg. Sci. Technol.*,**  
451 **18, 303–321, [https://doi.org/10.1016/0165-232X\(90\)90027-T](https://doi.org/10.1016/0165-232X(90)90027-T), 1990.**

452 Cole, D. M.: A model for the anelastic straining of saline ice subjected to cyclic loading, *Philos. Mag. A*, 72, 231–  
453 248, <https://doi.org/10.1080/01418619508239592>, 1995.

454 **Cole, D. M.: On the physical basis for the creep of ice: the high temperature regime. *J. Glaciol.*, 1–14.**  
455 **<https://doi.org/10.1017/jog.2020.15>, 2020.**

456 Cole, D. M. and Dempsey, J. P.: Influence of scale on the constitutive behavior of sea ice, In: International Union  
457 of Theoretical and Applied Mechanics Symposium on Scaling Laws in Ice Mechanics and Ice Dynamics,  
458 pp. 251–264. Kluwer, Dordrecht, [https://doi.org/10.1007/978-94-015-9735-7\\_22](https://doi.org/10.1007/978-94-015-9735-7_22), 2001.

459 Cole, D. M. and Dempsey, J. P.: In situ sea ice experiments in McMurdo Sound: cyclic loading, fracture, and  
460 acoustic emissions, *J. Cold Reg. Eng.*, 18, 155–174, [https://doi.org/10.1061/\(ASCE\)0887-](https://doi.org/10.1061/(ASCE)0887-381X(2004)18:4(155))  
461 **381X(2004)18:4(155)**, 2004.

462 Cole, D. M. and Durell, G. D.: The cyclic loading of saline ice, *Philos. Mag. A*, 72, 209–229,  
463 <https://doi.org/10.1080/01418619508239591>, 1995.



464 Cole, D. M. and Durell, G. D.: A dislocation-based analysis of strain history effects in ice, *Philos. Mag. A*, 81,  
465 1849–1872, <https://doi.org/10.1080/01418610108216640>, 2001.

466 Cole, D. M., Johnson, R. A., and Durell, G. D.: Cyclic loading and creep response of aligned first-year sea ice, *J.*  
467 *Geophys. Res.*, 103, 21,751–21,758S, <https://doi.org/10.1029/98JC01265>, 1998.

468 Dempsey, J. P.: Research trends in ice mechanics, *Int. J. Solids Struct.*, 37, 131–153,  
469 [https://doi.org/10.1016/S0020-7683\(99\)00084-0](https://doi.org/10.1016/S0020-7683(99)00084-0), 2000.

470 Dempsey, J. P., Adamson, R. M., and Mulmule. S. V.: Scale effects on the in-situ tensile strength and fracture of  
471 ice, Part II: First-year sea ice at Resolute, N.W.T. *Int. J. Fract.*, 95, 347–366,  
472 <https://doi.org/10.1023/A:1018650303385>, 1999.

473 Dempsey, J. P., Cole, D. M., and Wang, S.: Tensile fracture of a single crack in first-year sea ice. *Phil. Trans. R.*  
474 *Soc. A*, 376, <https://doi.org/10.1098/rsta.2017.0346>, 2018,

475 Eicken, H.: Salinity profiles of Antarctic sea ice: Field data and model results, *J. Geophys. Res.-Oceans*, 97,  
476 15,545–15,557, <https://doi.org/10.1029/92JC01588>, 1992.

477 Feltham, D. L.: sea Ice rheology. *Annu. Rev. Fluid Mech.*, 40, 91–112,  
478 <https://doi.org/10.1146/annurev.fluid.40.111406.102151>, 2008.

479 Gagne, M. E., Gillett N. P., and Fyfe, J. C.: Observed and simulated changes in Antarctic sea ice extent over the  
480 past 50 years, *Geophys. Res. Lett.*, 42, 90–95, <https://doi.org/10.1002/2014GL062231>, 2015.

481 Golden, K. M., Eicken, H., Heaton, A. L., Miner, J., Pringle, D. J., and Zhu, J.: Thermal evolution of permeability  
482 and microstructure in sea ice, *Geophys. Res. Lett.*, 34, L16501, <https://doi.org/10.1029/2007GL030447>,  
483 2007.

484 Gough, A. J., Mahoney, A. R., Langhorne, P. J., Williams, M. J. M., and Haskell, T. G.: Sea ice salinity and  
485 structure: A winter time series of salinity and its distribution, *J. Geophys. Res.-Oceans*, 7, C03008,  
486 <https://doi.org/10.1029/2011JC007527>, 2012.

487 **Gow, A. J. Crystalline structure of urea ice sheets used in modeling experiments in the CRREL test basin. CRREL**  
488 **report ; 84-24, <https://hdl.handle.net/11681/9553>, 1984.**

489 **Haskell, T. G., Robinson, W. H., and Langhorne, P. J.: Preliminary results from fatigue tests on in situ sea ice**  
490 **beams, *Cold Reg. Sci. Technol.*, 24, 167–176, [https://doi.org/10.1016/0165-232X\(95\)00015-4](https://doi.org/10.1016/0165-232X(95)00015-4), 1996.**

491 Heijkoop, A. N., Nord, T. S., and Høyland, K. V.: Strain-controlled cyclic compression of sea ice. 24th IAHR  
492 International Symposium on Ice Vladivostok, Russia, June 4 to 9, 2018.

493 Herman, A., Cheng, S., and Shen, H. H.: Wave energy attenuation in fields of colliding ice floes – Part 1: Discrete-  
494 element modelling of dissipation due to ice–water drag, *The Cryosphere*, 13, 2887–2900,  
495 <https://doi.org/10.5194/tc-13-2887-2019>, 2019a.

496 Herman, A., Cheng S., and Shen, H. H.: Wave energy attenuation in fields of colliding ice floes – Part 2: A  
497 laboratory case study, *The Cryosphere*, 13, 2901–2914, <https://doi.org/10.5194/tc-13-2901-2019>, 2019b.

498 Iliescu, D. and Schulson, E. M.: Brittle compressive failure of ice: monotonic versus cyclic loading, *Acta Mater.*,  
499 50, 2163–2172, [https://doi.org/10.1016/S1359-6454\(02\)00060-5](https://doi.org/10.1016/S1359-6454(02)00060-5), 2002.

500 Iliescu, D., Murdza, A., Schulson, E. M., and Renshaw, C. E.: Strengthening ice through cyclic loading, *J. Glaciol.*,  
501 63, 663–669, <https://doi.org/10.1017/jog.2017.32>, 2017.

502 Jones, K. A., Ingham, M., and Eicken, H. Modeling the anisotropic brine microstructure in first - year arctic sea  
503 ice, *J. Geophys. Res.-Oceans*, 117, C02005, doi:10.1029/2011JC007607, 2012.

504 Kartashkin, B. D.: Experimental studies of the physico-mechanical properties of ice, Tsentra'nyy  
505 Aerogidrodinamicheskiy Institut, 1947

506 Kern, S., Lavergne, T., Notz, D., Pedersen, L. T., Tonboe, R. T., Saldo, R., and Sørensen, A. M. D.: Satellite passive  
507 microwave sea-ice concentration data set intercomparison: closed ice and ship-based observations, *The*  
508 *Cryosphere*, 13, 3261–3307, <https://doi.org/10.5194/tc-13-3261-2019>, 2019.

509 Langway, C. C.: Ice fabrics and the universal stage, Report # 62, CRREL, 1958.

510 Langhorne, P. J., Squire, V. A., Fox, C., and Haskell, T. G.: Break-up of sea ice by ocean waves, *Ann. Glaciol.*, 27,  
511 438–442, <https://doi.org/10.3189/S0260305500017869>, 1998.

512 Langhorne, P. J., Hughes, K. G., Gough, A. J., Smith, I. J., Williams, M. J. M., Robinson, N. J., Stevens, C. L.,  
513 Rack, W., Price, D., Leonard, G. H., Mahoney, A. R., Haas, C., and Haskell, T. G.: Observed platelet ice  
514 distributions in Antarctic sea ice: An index for ocean-ice shelf heat flux, *Geophys. Res. Lett.*, 42, 5442–  
515 5451, <https://doi.org/10.1002/2015GL064508>, 2015.

516 Leclair, E. S., Schapery, R. A., and Dempsey, J. P.: A broad-spectrum constitutive modeling technique applied to  
517 saline ice, *Int. J. Fract.*, 97, 209–226, <https://doi.org/10.1023/A:1018358923672>, 1999.

518 Li, J., Kohout, A. L., and Shen, H. H.: Comparison of wave propagation through ice covers in calm and storm  
519 conditions, *Geophys. Res. Lett.*, 42, 5935–5941, <https://doi.org/10.1002/2015GL064715>, 2015.

520 Li, Z., Riska, K.: Preliminary study of physical and mechanical properties of model ice. Technical Report M-212.  
521 Helsinki University of Technology, 1996.

522 Liu, Y., Dai, F., Dong, L., Xu N., and Feng, P.: Experimental investigation on the fatigue mechanical properties of  
523 intermittently jointed rock models under cyclic uniaxial compression with different loading parameters,  
524 *Rock Mech. Rock Eng.*, 51, 47–68, <https://doi.org/10.1007/s00603-017-1327-7>, 2018.

525 Liu, Y., Dai, F., Fan, P., Xu, N., and Dong, L.: Experimental investigation of the influence of joint geometric  
526 configurations on the mechanical properties of intermittent jointed rock models under cyclic uniaxial  
527 compression, *Rock Mech. Rock Eng.*, 50, 453–1471, <https://doi.org/10.1007/s00603-017-1190-6>, 2017

528 Lu, W. and Løset, S.: Parallel channels' fracturing mechanism during ice management operations. Part II:  
529 Experiment, *Cold Reg. Sci. Technol.*, 156, 117–133, <https://doi.org/10.1016/j.coldregions.2018.07.011>,  
530 2018.

531 Lu, W., Lubbad, R., Shestov, A., and Løset, S.: Parallel channels' fracturing mechanism during ice management  
532 operations, Part I: Theory. *Cold Reg. Sci. Technol.*, 156, 102–116,  
533 <https://doi.org/10.1016/j.coldregions.2018.07.010>, 2018.

534 Marchenko, A. and Lishman, B.: The influence of closed brine pockets and permeable brine channels on the  
535 thermo-elastic properties of saline ice. *Phil. Trans. R. Soc. A*, 375, 20150351,  
536 <http://dx.doi.org/10.1098/rsta.2015.0351>, 2017.

537 Mellor, M. and Cole, D.: Cyclic loading and fatigue in ice. *Cold Reg. Sci. Technol.*, 4, 41-53,  
538 [https://doi.org/10.1016/0165-232X\(81\)90029-X](https://doi.org/10.1016/0165-232X(81)90029-X), 1981.

539 Murdza, A., Schulson, E. M., and Renshaw, C. E.: Hysteretic behavior of freshwater ice under cyclic loading: A  
540 preliminary results. 24th IAHR International Symposium on Ice. Vladivostok, 185–192, 2018.

541 Murdza, A., Schulson, E. M., and Renshaw, C. E.: The effect of cyclic loading on the flexural strength of columnar  
542 freshwater ice. In the Proceedings of the 25th International Conference on Port and Ocean Engineering  
543 under Arctic Conditions (POAC'19). Electronic publication, 2019.

544 O'Connor DT, West BA, Haehnel RB, Asenath-Smith E, Cole D. A viscoelastic integral formulation and numerical  
545 implementation of an isotropic constitutive model of saline ice, *Cold Reg. Sci. Technol.*, 171, 102983,  
546 <https://doi.org/10.1016/j.coldregions.2019.102983>, 2020.

547 Polojärvi, A., Tuhkuri, J., and Pustogvar, A. DEM simulations of direct shear box experiments of ice rubble: Force  
548 chains and peak loads, *Cold Reg. Sci. Technol.*, 116, 12–23,  
549 <https://doi.org/10.1016/j.coldregions.2015.03.011>, 2015.

550 Ranta, J., Polojärvi, A., and Tuhkuri, J. The statistical analysis of peak ice loads in a simulated ice-structure  
551 interaction process, *Cold Reg. Sci. Technol.*, 133, 46–55,  
552 <https://doi.org/10.1016/j.coldregions.2016.10.002>, 2017.

553 Ranta, J., Polojärvi, A., and Tuhkuri, J.: Ice loads on inclined marine structures - Virtual experiments on ice failure  
554 process evolution, *Mar. Struct.*, 57, 72–86, <https://doi.org/10.1016/j.marstruc.2017.09.004>, 2018a.

555 Ranta, J., Polojärvi, A., and Tuhkuri, J.: Limit mechanisms for ice loads on inclined structures: Buckling, *Cold*  
556 *Reg. Sci. Technol.*, 147, 34–44, <https://doi.org/10.1016/j.coldregions.2017.12.009>, 2018b.

557 Reistad, M., Breivik, Ø., Haakenstad, H., Aarnes, O. J., Furevik, B. R., and Bidlot, J. R.: A high-resolution hindcast  
558 of wind and waves for the North Sea, the Norwegian Sea, and the Barents Sea, *J. Geophys. Res.*, 116,  
559 C05019, <https://doi.org/10.1029/2010JC006402>, 2011.

560 Ridley, J. K. and Blockley, E. W.: Brief communication: Solar radiation management not as effective as CO<sub>2</sub>  
561 mitigation for Arctic sea ice loss in hitting the 1.5 and 2 °C COP climate targets, *The Cryosphere*, 12,  
562 3355–3360, <https://doi.org/10.5194/tc-12-3355-2018>, 2018.

563 Schulson, E. M. and Duval, P.: *Creep and fracture of ice*, Cambridge University Press, Cambridge, 2009.

564 Serreze, M. C. and Stroeve, J.: Arctic sea ice trends, variability and implications for seasonal ice forecasting, *Phil.*  
565 *Trans. R. Soc. A*, 373, 20140159, <http://dx.doi.org/10.1098/rsta.2014.0159>, 2015.

566 Smith, I. J., Gough, A. J., Langhorne, P. J., Mahoney, A. R., Leonard, G. H., Van Hale, R., Jendersie, S., and  
567 Haskell, T. G.: First-year land-fast Antarctic sea ice as an archive of ice shelf meltwater fluxes, *Cold*  
568 *Reg. Sci. Technol.*, 113, 63–70, <https://doi.org/10.1016/j.coldregions.2015.01.007>, 2015.

569 Tabata, T. and Nohguchi, Y.: Failure of sea ice by repeated compression, In: Tryde P. (eds) *Physics and Mechanics*  
570 *of Ice*, International Union of Theoretical and Applied Mechanics, Springer, Berlin, Heidelberg, 351–362,  
571 [https://doi.org/10.1007/978-3-642-81434-1\\_25](https://doi.org/10.1007/978-3-642-81434-1_25), 1980.

572 Timco, G. W. and Weeks, W. F.: A review of the engineering properties of sea ice, *Cold Reg. Sci. Technol.*, 60,  
573 107–129, <https://doi.org/10.1016/j.coldregions.2009.10.003>, 2010.

574 Tuhkuri, J. and Polojärvi, A.: A review of discrete element simulation of ice-structure interaction, *Phil. Trans. R.*  
575 *Soc. A*, 376, 20170335, <http://dx.doi.org/10.1098/rsta.2017.0335>, 2018.

576 Vincent, M. R. and Dempsey, J. P.: Servo-hydraulic pin loading device (HPLD) for in situ ice testing, *J. Cold Reg.*  
577 *Eng.*, 13, 21–36, [https://doi.org/10.1061/\(ASCE\)0887-381X\(1999\)13:1\(21\)](https://doi.org/10.1061/(ASCE)0887-381X(1999)13:1(21)), 1999.

578 Voermans, J. J., Babanin, A. V., Thomson, J., Smith, M. M., and Shen, H. H.: Wave attenuation by sea ice  
579 turbulence, *Geophys. Res. Lett.*, 46, 6796–6803, <https://doi.org/10.1029/2019GL082945>, 2019.

580 Weber, L. J. and Nixon, W. A.: Hysteretic behavior in ice under fatigue loading. *Proceedings of the 15th*  
581 *International Conference on Offshore Mechanics and Arctic Engineering*. 75–82, 1996.

582 Wongpan, P., Hughes, K. G., Langhorne, P. J., and Smith, I. J.: Brine Convection, temperature fluctuations, and  
583 permeability in winter Antarctic land-fast sea ice, 123, 216–230, <https://doi.org/10.1002/2017JC012999>,  
584 2018.

585 Zijlema, M., Vledder, G. Ph. van, and Holthuijsen, L. H.: Bottom friction and wind drag for wave models, *Coast.*  
586 *Eng.*, 65, 19–26, <https://doi.org/10.1016/j.coastaleng.2012.03.002>, 2012.

587

588

589 **Table 1** The test matrix of this experimental campaign. The campaign included two test types, two ice  
 590 salinities, five periods and two test-type-dependent load levels. For each case, two specimens harvested from  
 591 two ice sheets were tested.

Case	Specimen no.	Ice salinity (ppt)	Dry/Floating	Average ice temperature (°C)	Period (s)	Cyclic compressive Stresses (MPa)
I	Dry-5ppt-1, Dry-5ppt-2	5	Dry	-10	1, 5, 10, 100, 500, 1000	0.08–0.25
II	Dry-7ppt-1, Dry-7ppt-2	7	Dry	-10	1, 5, 10, 100, 500, 1000	0.08–0.25
III	Floating-5ppt-1, Floating-5ppt-2	5	Floating	-2.5	1, 5, 10, 100, 500, 1000	0.04–0.12
IV	Floating-7ppt-1, Floating-7ppt-2	7	Floating	-2.5	1, 5, 10, 100, 500, 1000	0.04–0.12

592

593 **Table 2** The energy density ( $\text{J}\cdot\text{m}^{-3}$ ) dissipated in a typical loading-unloading cycle of each experiment.

Specimen no.	Frequency (Hz)				
	0.001	0.002	0.01	0.1	0.2
Dry-5ppt-1	8.83	5.44	2.01	0.67	0.71
Dry-5ppt-2	5.36	2.93	1.57	0.54	0.36
Dry-7ppt-1	14.4	7.16	2.87	0.91	0.66
Dry-7ppt-2	20.8	14.0	7.80	2.49	2.05
Floating-5ppt-1	25.0	15.4	4.78	0.85	0.63
Floating-5ppt-2	28.4	16.2	4.79	0.91	0.54
Floating-7ppt-1	151	67.7	20.2	3.85	2.52
Floating-7ppt-2	63.6	38.3	11.7	2.40	1.63

594

595 **Table 3** The energy dissipation rate (%) in a typical loading-unloading cycle of each experiment.

Specimen no.	Frequency (Hz)				
	0.001	0.002	0.01	0.1	0.2
Dry-5ppt-1	48.3	40.2	22.0	9.86	9.93
Dry-5ppt-2	35.4	22.7	17.6	8.68	5.50
Dry-7ppt-1	55.6	37.3	21.6	11.0	8.60
Dry-7ppt-2	55.7	44.7	32.3	16.0	14.3
Floating-5ppt-1	89.6	76.1	44.2	15.5	11.8
Floating-5ppt-2	87.7	69.8	39.4	17.4	11.3
Floating-7ppt-1	98.3	91.7	70.5	32.0	25.1
Floating-7ppt-2	88.1	76.0	56.4	26.3	20.2

596  
597

**Table 4. Values of the model parameters calibrated for simulating the strain response of the ice specimens (in Section 5, these values are discussed and compared to those reported in references).**

Specimen no.	Elastic modulus $E_0$ (GPa)	Dislocation density $\rho$ ( $m^{-2}$ )	Strength of dislocation relaxation $\delta D^d$ ( $Pa^{-1}$ )	Strength of grain boundary $\delta D^{gb}$ ( $Pa^{-1}$ )
Dry-5ppt-1	6.0	$7.53 \times 10^8$	$7 \times 10^{-10}$	$1 \times 10^{-10}$
Dry-5ppt-2	5.6	$4.31 \times 10^8$	$4 \times 10^{-10}$	$1 \times 10^{-10}$
Dry-7ppt-1	4.0	$1.18 \times 10^9$	$1.1 \times 10^{-9}$	$1 \times 10^{-10}$
Dry-7ppt-2	4.0	$1.83 \times 10^9$	$1.7 \times 10^{-9}$	$3 \times 10^{-10}$
Floating-5ppt-1	2.0	$5.92 \times 10^9$	$5.5 \times 10^{-9}$	$3 \times 10^{-10}$
Floating-5ppt-2	1.9	$6.46 \times 10^9$	$6 \times 10^{-9}$	$1 \times 10^{-10}$
Floating-7ppt-1	1.9	$2.58 \times 10^{10}$	$2.4 \times 10^{-8}$	$3 \times 10^{-10}$
Floating-7ppt-2	1.7	$1.40 \times 10^{10}$	$1.3 \times 10^{-8}$	$2 \times 10^{-10}$

598  
599  
600

**Table 5. Modeling results of the strain energy density ( $J \cdot m^{-3}$ ) dissipated per loading-unloading cycle (the values given in parentheses are error percentages of model predictions relative to experimental results).**

Specimen no.	Frequency				
	0.001 Hz	0.002 Hz	0.01 Hz	0.1 Hz	0.2 Hz
Dry-5ppt-1	9.12 (7%)	5.16 (9%)	1.74 (-10%)	0.69 (-9%)	0.68 (-21%)
Dry-5ppt-2	5.22 (-3%)	3.10 (6%)	1.15 (-27%)	0.55 (2%)	0.33 (-8%)
Dry-7ppt-1	15.1 (5%)	8.76 (22%)	2.65 (-8%)	0.86 (-5%)	0.79 (20%)
Dry-7ppt-2	21.9 (-1%)	12.5 (-4%)	6.44 (-9%)	2.00 (-22%)	1.97 (12%)
Floating-5ppt-1	27.0 (8%)	14.9 (-3%)	4.05 (-15%)	0.91 (7%)	0.73 (16%)
Floating-5ppt-2	30.3 (3%)	16.8 (1%)	4.58 (-6%)	0.89 (-17%)	0.61 (-8%)
Floating-7ppt-1	125 (-17%)	68.5 (1%)	18.6 (-8%)	3.79 (-2%)	2.58 (2%)
Floating-7ppt-2	65.4 (-17%)	36.4 (-4%)	10.0 (-21%)	2.18 (10%)	1.73 (13%)

601  
602  
603  
604  
605

606

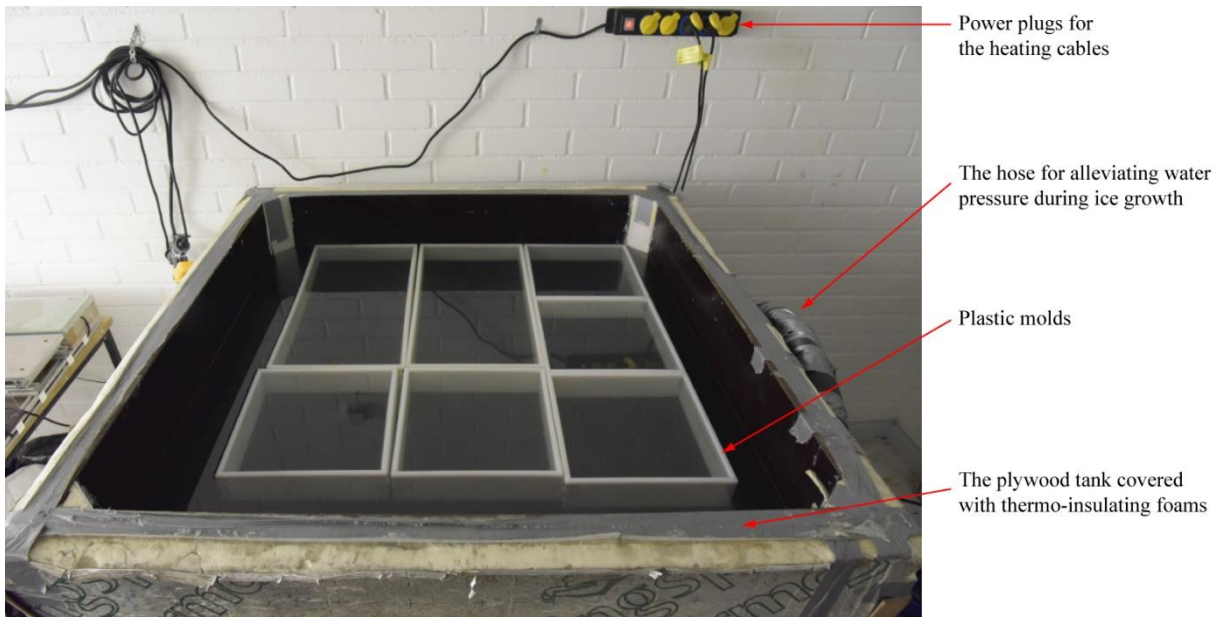
607

**Table 6. Modeling results of the strain energy dissipation rate (%) per loading-unloading cycle (the values given in parentheses are error percentages of model predictions relative to experimental results).**

Specimen no.	Frequency				
	0.001 Hz	0.002 Hz	0.01 Hz	0.1 Hz	0.2 Hz
Dry-5ppt-1	49.2 (4%)	36.7 (-1%)	18.5 (-13%)	9.43 (-12%)	9.81 (-16%)
Dry-5ppt-2	37.4 (16%)	25.9 (14%)	13.9 (-21%)	7.5 (-5%)	5.70 (12%)
Dry-7ppt-1	53.1 (-1%)	41.3 (-2%)	20.2 (10%)	8.99 (-18%)	8.50 (12%)
Dry-7ppt-2	51.3 (-1%)	38.9 (-2%)	25.7 (10%)	12.6 (-18%)	13.9 (12%)
Floating-5ppt-1	87.8 (-5%)	77.1 (-4%)	40.0 (-15%)	16.0 (3%)	14.0 (3%)
Floating-5ppt-2	91.1 (-1%)	82.0 (6%)	45.1 (-4%)	17.6 (9%)	13.4 (26%)
Floating-7ppt-1	86.4 (-1%)	77.4 (-3%)	59.9 (-10%)	34.0 (13%)	28.2 (17%)
Floating-7ppt-2	94.5 (-1%)	88.3 (-3%)	52.9 (-10%)	23.8 (13%)	20.5 (17%)

608

609



610

**Figure 1. The tank made of plywood for growing ice specimens.**

611



(a)

(b)

612

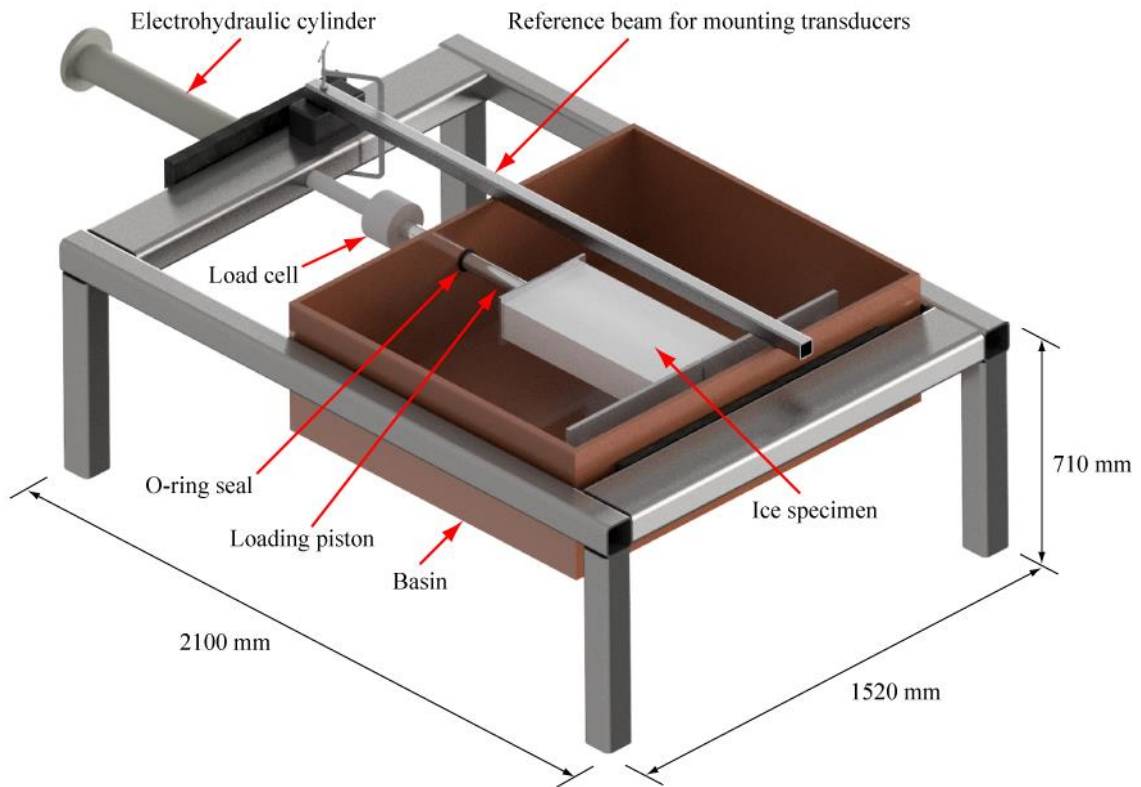
**Figure 2. Equipment used in the (a) dry and (b) floating ice experiments. One of the plastic molds used when growing ice is shown in (b). The thin ice cover of the basin, seen in (b), was broken before performing the experiments.**

615

616

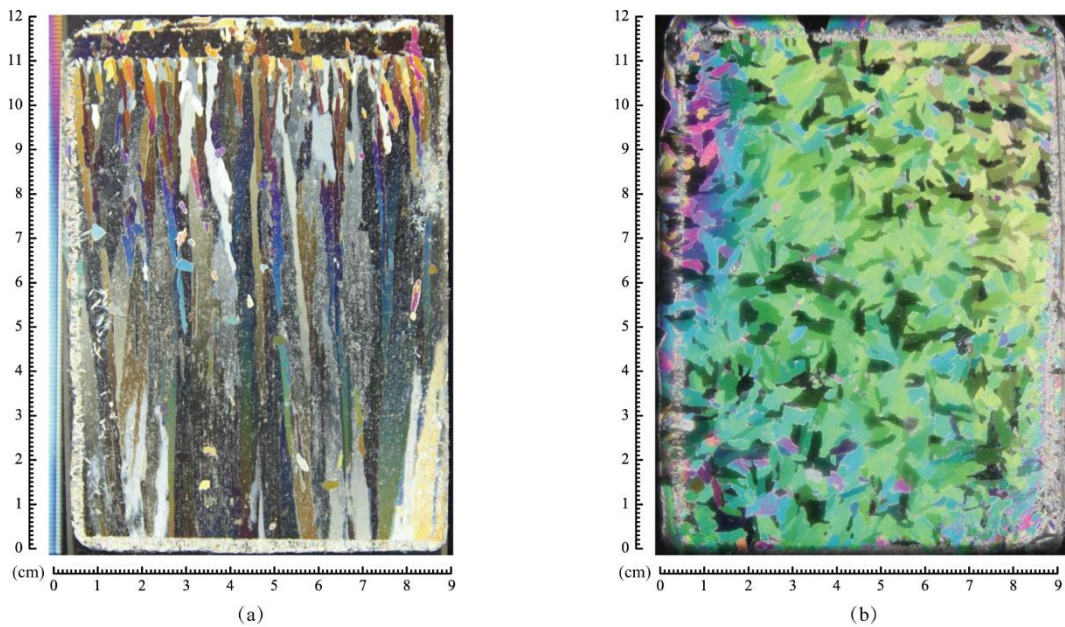


617



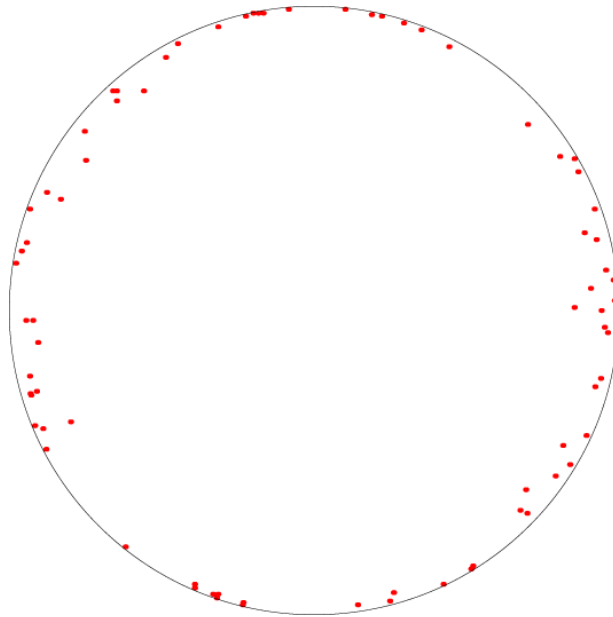
618 **Figure 3. A sketch of the test rig used in the experiments. The inner dimensions of the basin are 1320 mm ×**  
619 **1280 mm × 400 mm.**

620



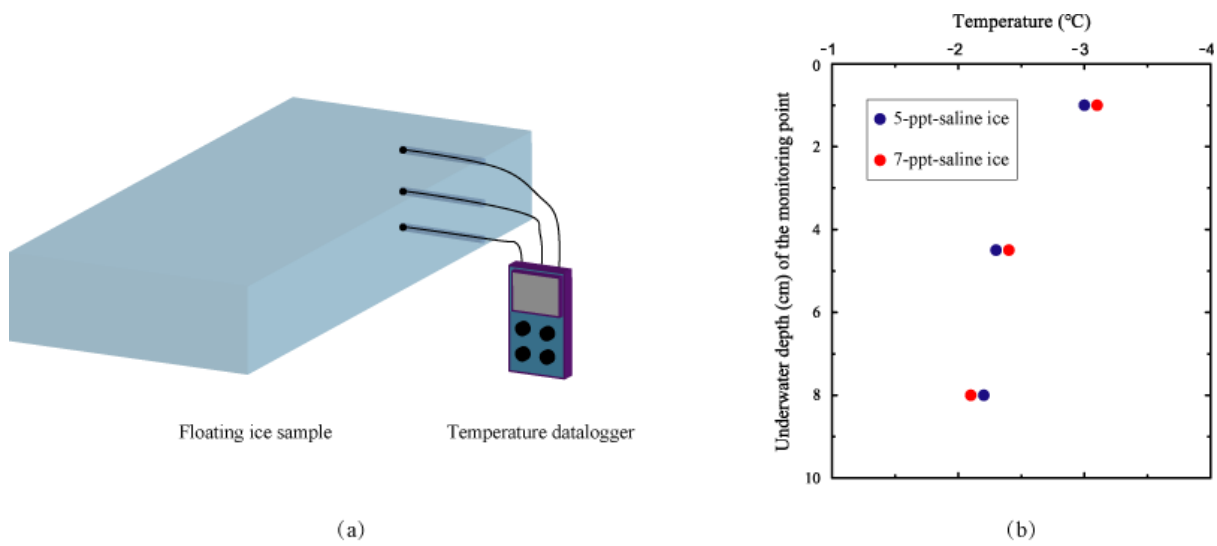
621 **Figure 4. One set of thin sections of the ice (salinity: 5 ppt) grown in this experimental campaign: (a) vertical;**  
622 **(b) horizontal.**

624



625  
626  
627  
628

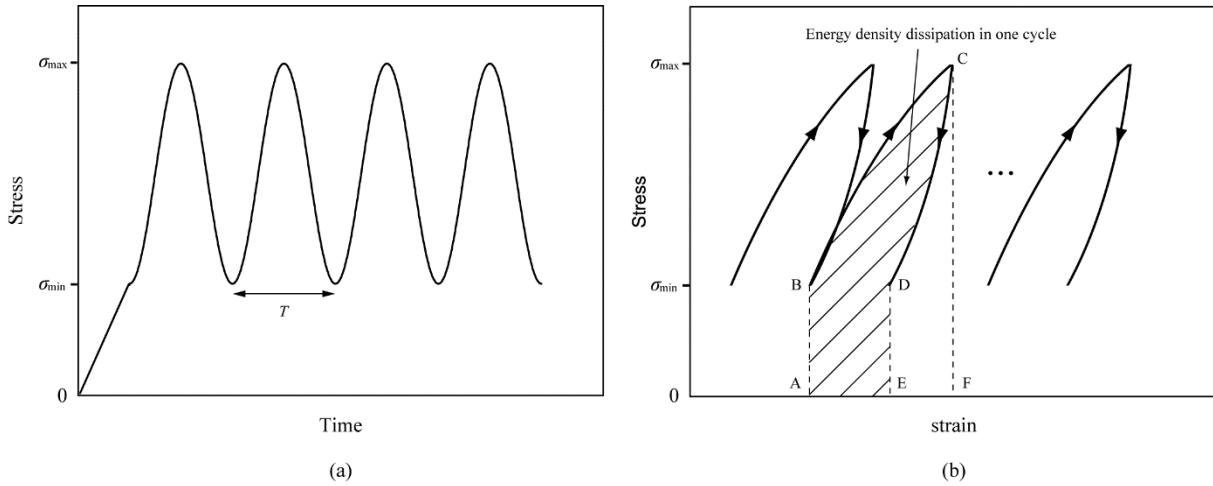
Figure 5. A typical Schmidt equal area net pole projection drawn on the basis of grain orientations.



629  
630  
631  
632

Figure 6. Monitoring of the through-thickness thermal gradient of floating ice: (a) a schematic diagram of the arrangement of the temperature probes and (b) the measured through-thickness thermal gradient inside two floating ice specimens.

633



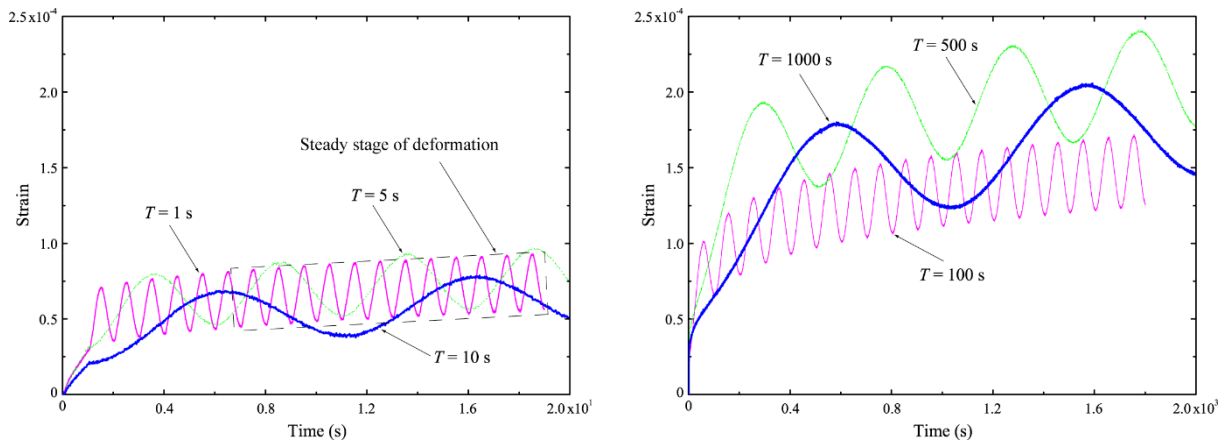
634

**Figure 7. Schematic diagrams of the cyclic loads: (a) the inputted stress waveform, and (b) the method for calculating the energy density dissipated in one loading cycle (in other words, region ABCDE).**

635

636

637



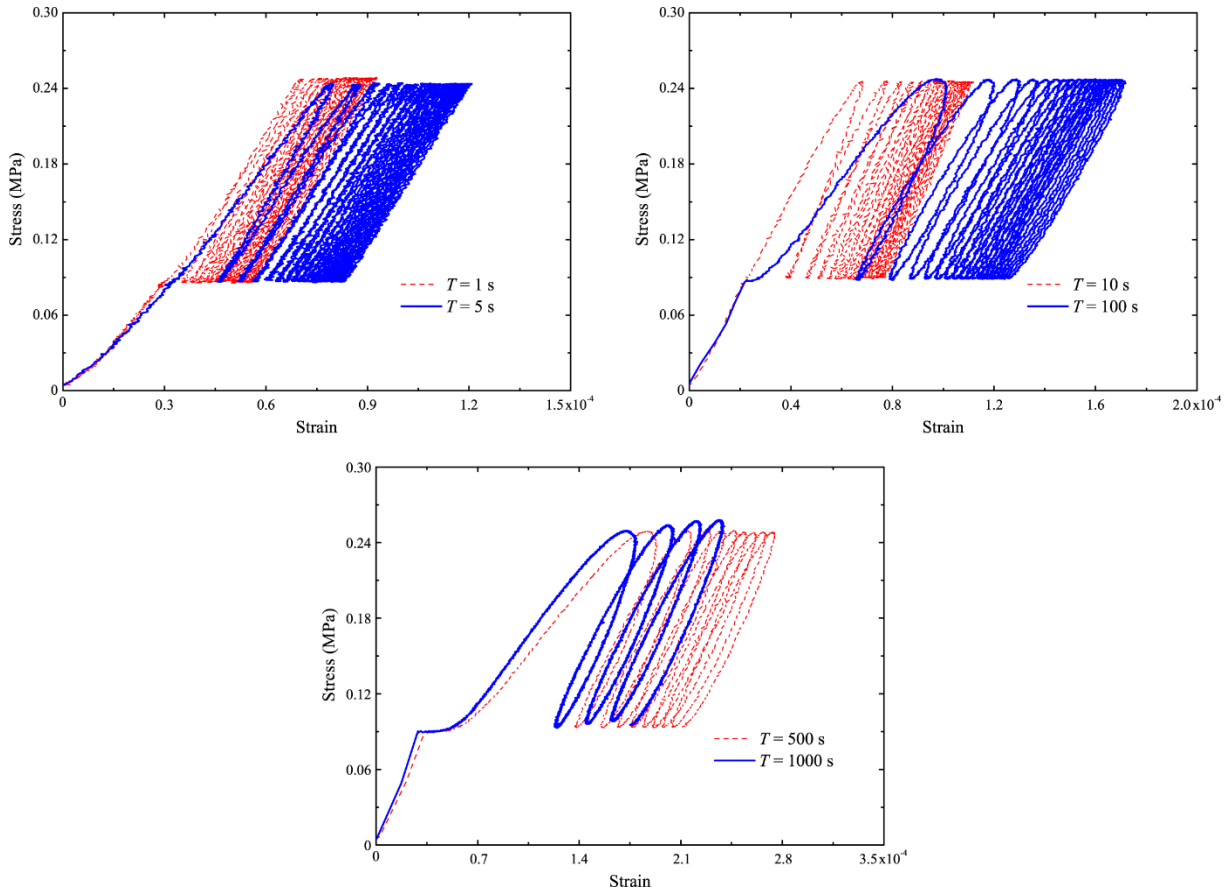
638

**Figure 8. Strain-time curves of specimen Dry-5ppt-1 tested with stresses varying from 0.08 to 0.25 MPa and with the temperature of -10°C.**

639

640

641

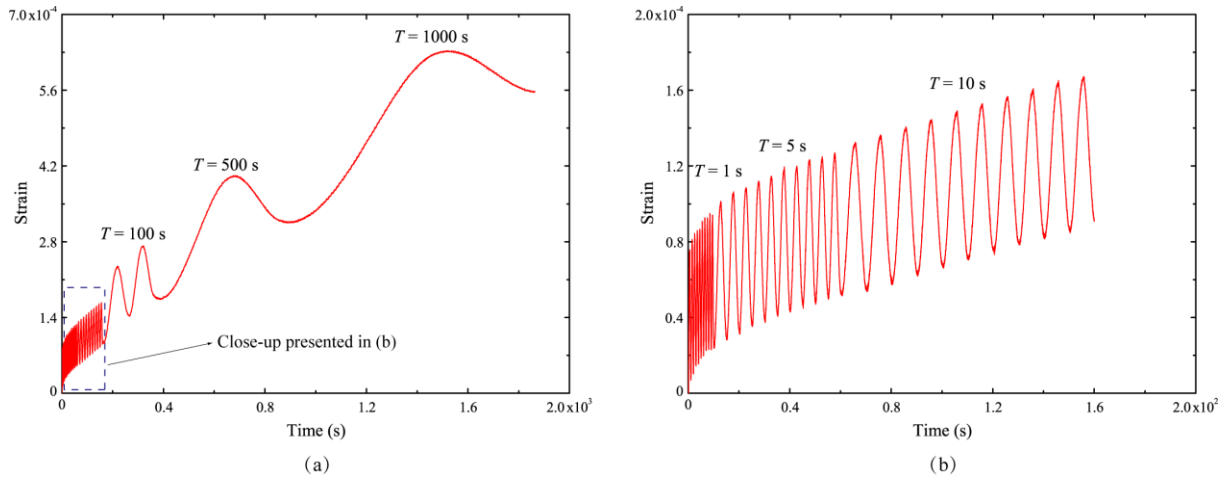


642

643 **Figure 9. Stress-strain curves of specimen Dry-5ppt-1 tested with stresses varying from 0.08 to 0.25 MPa**  
644 **and with the temperature of -10°C.**

644

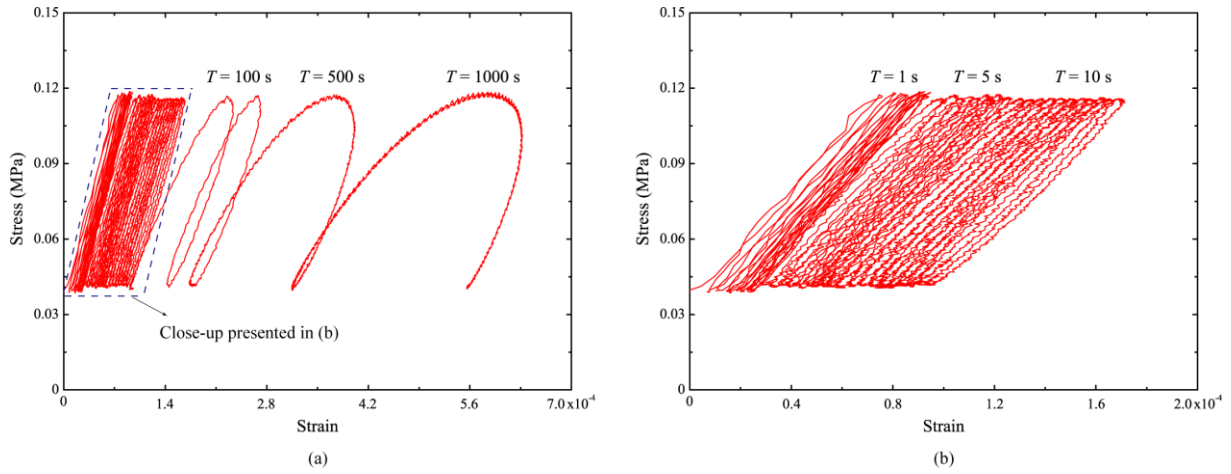
645



646

647 **Figure 10. Strain response of specimen Floating-5ppt-1 tested with stresses varying from 0.04 to 0.12 MPa**  
648 **and with the average temperature of -2.5°C: (a) shows the response for all periods,  $T$ , of cyclic loading, while**  
649 **(b) presents a close-up showing the cycles for  $T = 1, 5$  and  $10$  s.**

650

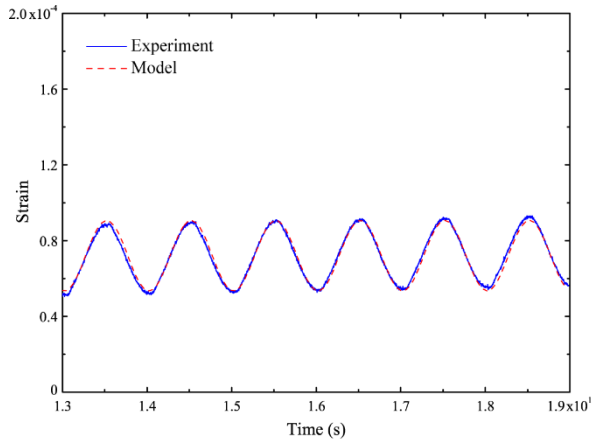
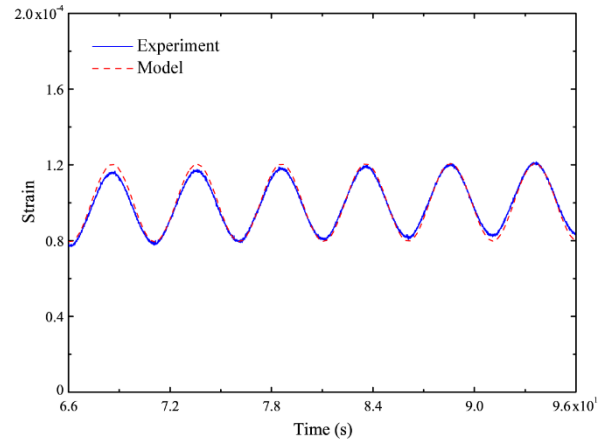
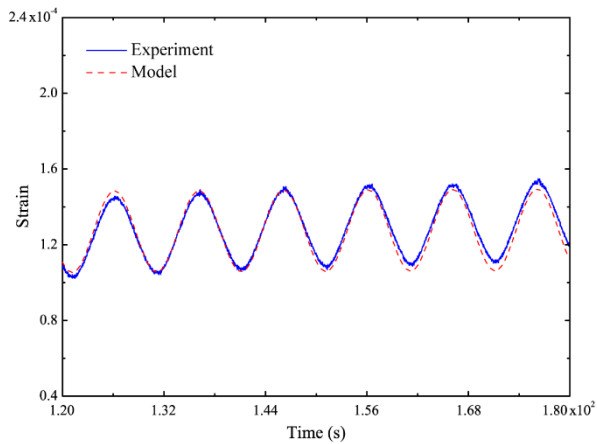
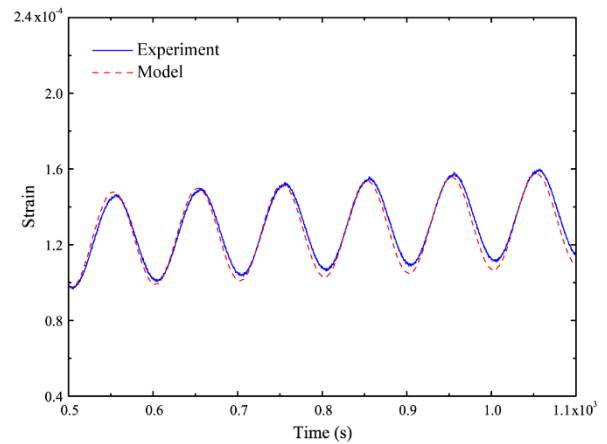
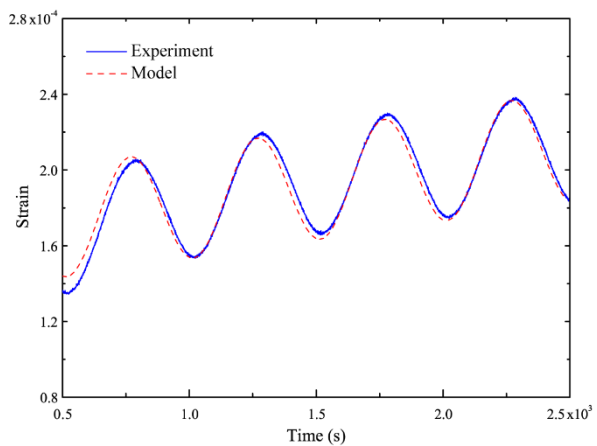
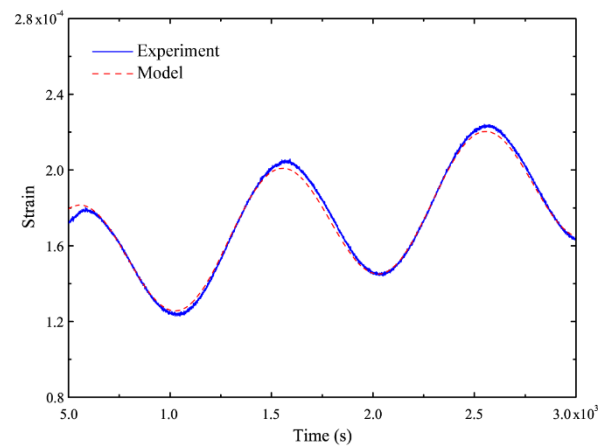


651

652

653

**Figure 11. Stress-strain plots of specimen Floating-5ppt-1 tested with stresses varying from 0.04 to 0.12 MPa and with the average temperature of  $-2.5^{\circ}\text{C}$ : (a) shows the response for all periods,  $T$ , of cyclic loading, while (b) presents a close-up showing the cycles for  $T = 1, 5$  and  $10$  s.**

(a)  $T = 1$  s(b)  $T = 5$  s(c)  $T = 10$  s(d)  $T = 100$  s(e)  $T = 500$  s(f)  $T = 1000$  s

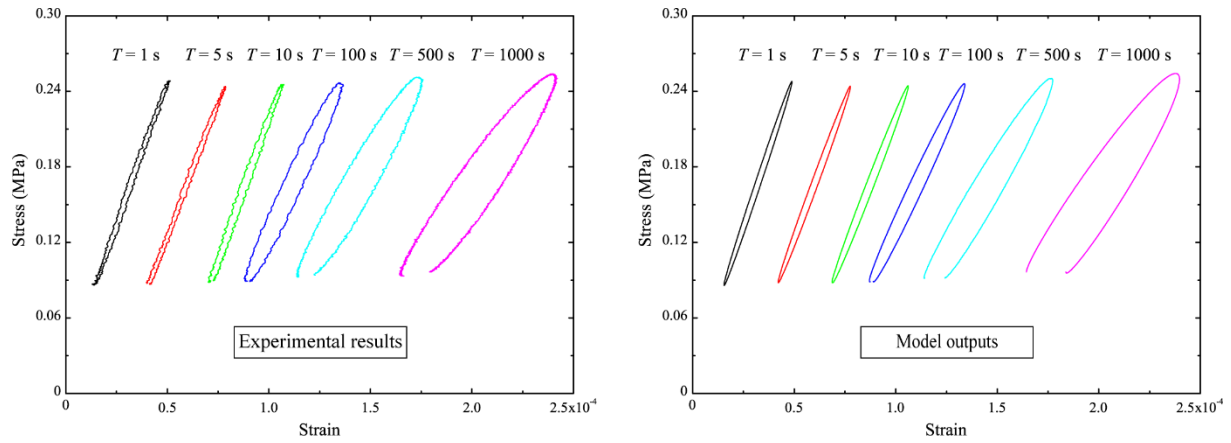
655

656

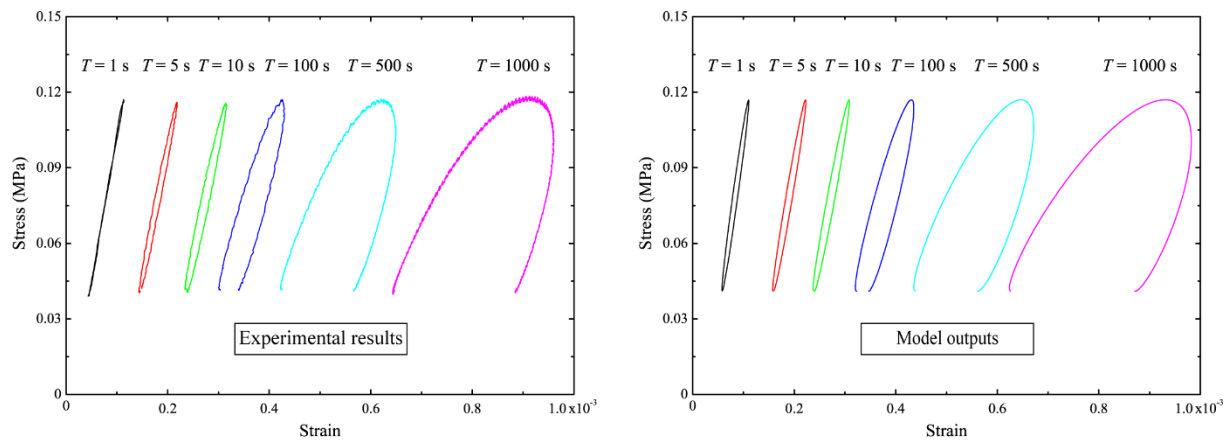
657

**Figure 12. Comparison between the experimentally measured strain-time curves (in the steady stage) and the results yielded by the physically based model for specimen Dry-5ppt-1 tested with stresses varying from 0.08 to 0.25 MPa and with the temperature of  $-10^{\circ}\text{C}$ .**

658



(a)



(b)

659

660

661

662

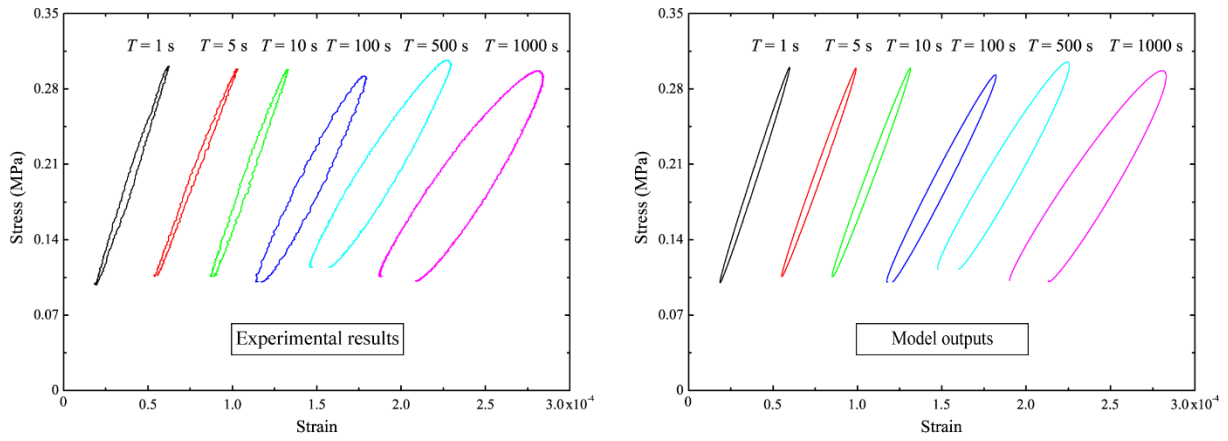
663

664

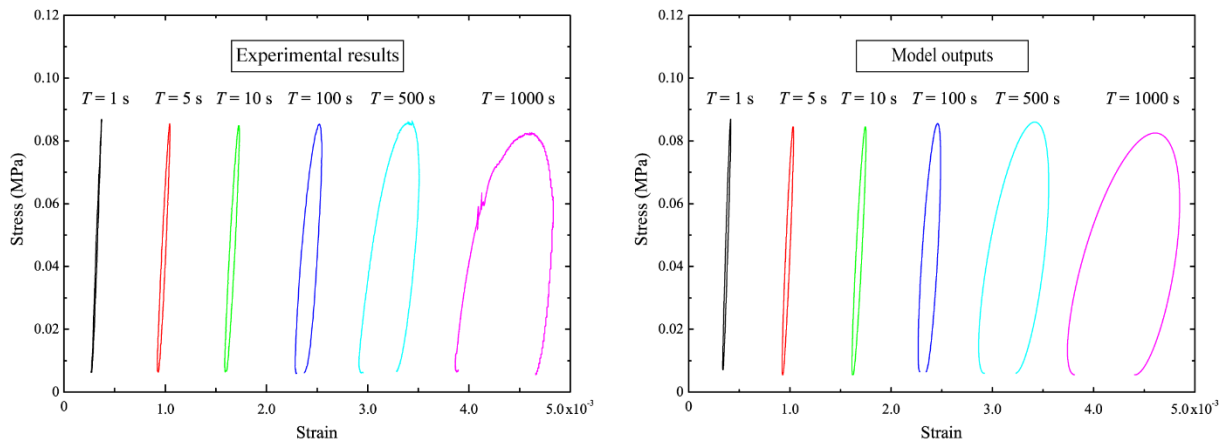
665

666

**Figure 13. Comparison between the steady-state stress-strain hysteresis loop measured in the experiments and that outputted from the model for (a) specimen Dry-5ppt-1 with the temperature of  $-10^{\circ}\text{C}$  and (b) specimen Floating-5ppt-1 with the average temperature of  $-2.5^{\circ}\text{C}$  (note that, to compare the representative hysteresis loops in all the different-frequency experiments with those outputted by the model in a more concise and intuitive way, the pre-strains before the hysteresis loops drawn here are not equal to the experimental values).**



(a)



(b)

667  
668

669

670

671

672

673

674

675

**Figure 14. Comparison between the steady-state stress-strain hysteresis loops measured in the experiments and those predicted by the dislocation-based model for (a) specimen Dry-5ppt-1 tested with stresses varying from 0.1 to 0.3 MPa and with the temperature of  $-10^{\circ}\text{C}$  and (b) specimen Floating-5ppt-1 tested with stresses varying from 0.005 to 0.085 MPa and with the average temperature of  $-2.5^{\circ}\text{C}$  (note that, to compare the representative hysteresis loops in all the different-frequency experiments with those outputted by the model in a more concise and intuitive way, the pre-strains before the hysteresis loops drawn here are not equal to the experimental values).**